INTERNATIONAL ATOMIC ENERGY AGENCY

INDC(NDS)-462
Distr: G+NM

I N D C INTERNATIONAL NUCLEAR DATA COMMITTEE

Parameters for Calculation of Nuclear Reactions of Relevance to Non-Energy Nuclear Applications

(Reference Input Parameter Library: Phase III)

Summary Report of the First Research Coordination Meeting

IAEA Headquarters
Vienna, Austria
23 – 25 June 2004

Prepared by

R. Capote Noy
IAEA Nuclear Data Section
Vienna, Austria

August 2004

Produced by the IAEA in Austria
August 2004

INDC(NDS)-462
Distr.: G+NM

Parameters for Calculation of Nuclear Reactions of Relevance to Non-Energy Nuclear Applications

(Reference Input Parameter Library: Phase III)

Summary Report of the First Research Coordination Meeting

IAEA Headquarters
Vienna, Austria
23 – 25 June 2004

Prepared by

R. Capote Noy
IAEA Nuclear Data Section
Vienna, Austria

Abstract

A summary is given of the First Research Coordination Meeting on Parameters for Calculation of Nuclear Reactions of Relevance to Non-Energy Nuclear Applications (Reference Input Parameter Library: Phase III), including a critical review of the RIPL-2 file. The new library should serve as input for theoretical calculations of nuclear reaction data at incident energies up to 200 MeV, as needed for energy and non-energy modern applications of nuclear data. Technical discussions and the resulting work plan of the Coordinated Research Programme are summarized, along with actions and deadlines. Participants' contributions to the RCM are also attached.

August 2004

TABLE OF CONTENTS

SUMMARY OF THE MEETING

With recent formulations of nuclear reaction statistical models, nuclear reaction theory is believed to be in a position to meet most of the requirements for practical applications. The major sources of uncertainty are the input parameters needed to perform theoretical calculations. The IAEA has addressed these needs through a series of Co-ordinated Research Projects (CRP) on the Reference Input Parameter Library (RIPL), which involves the difficult task of collecting, evaluating and recommending the vast amounts of various nuclear parameters. RIPL is targeted at users of nuclear reaction codes and, in particular, at nuclear data evaluators. The first phase of the project was completed in 1999, with the production of a Starter File and related documentation (IAEA-TECDOC 1034)[1]. A second phase of the project was finished in 2002[2]. Substantial improvements and extensions to the Starter File have been made, resulting in a more accurate and reliable library. All files selected for RIPL-2 have been prepared in the unified RIPL-2 format, which facilitates their use in the reaction codes. The RIPL-2 library was released in July 2002 and is available on the web (http://www-nds.iaea.org/RIPL-2/). RIPL-2 constitutes a comprehensive and consistent set of nuclear reaction input parameters but its scope is limited to neutron-induced reactions up to 20 MeV, i.e., to a range typical for conventional power reactors. Addressing needs of other emerging nuclear technologies require extension of the RIPL-2 database to cover model parameters for calculation of nuclear reactions needed for non-energy applications such as: accelerator driven waste incineration, production of radioisotopes for therapy and diagnostics, charged particle beam therapy, and material analysis. In addition, there is a worldwide interest in nuclear astrophysics, which is constrained to rely on theoretical calculations of nuclear reaction cross sections to model distribution of isotopes in the Universe. To fulfil these requirements, the third and final phase of the RIPL project named "Parameters for calculation of nuclear reactions of relevance to non-energy nuclear applications" began in 2003.

The first Research Coordination Meeting (RCM) of the RIPL-3 CRP was held at IAEA Headquarters, Vienna (Austria) between 23 - 25 June 2004, and attended by seven CRP participants, three external consultants with Prof. H. Leeb as a local observer from the Technical University of Vienna. The IAEA was represented by A.L. Nichols (Head, Nuclear Data Section), A. Trkov, V. Pronyaev and R. Capote, who served as Scientific Secretary. M. Herman (BNL) was elected Chairman of the meeting. The approved Agenda is attached (Appendix 1) as well as a list of participants and their affiliations (Appendix 2).

Prior to the meeting, the assignment of tasks related to each of the RIPL segments was discussed by e-mail between the participants and Scientific Secretary. The participants reviewed the status of the work within the CRP and discussed scientific and technical details. In particular, issues related to level densities, optical model for deformed nuclei, fission barriers and parameter uncertainties were debated in detail. Contributions to the meetings by participants are attached (Appendix 3). The participants agreed to undertake efforts to ensure internal consistency and completeness of the library. The general structure of the RIPL database is well established and will remain unchanged. The expected output of the CRP will

---

[1]Handbook for calculations of nuclear reaction data: Reference input parameter library (International Atomic Energy Agency, Vienna, Austria, 1998), **IAEA-TECDOC-1034.**

[2]Handbook for calculations of nuclear reaction data: Reference input parameter library RIPL-2 (International Atomic Energy Agency, Vienna, Austria, 2004), IAEA-TECDOC-to be published.

be an updated and expanded electronic database based on the RIPL-2 database. Some changes are expected in order to accommodate additional information needed for non-energy applications.

The main goals to be achieved within the new project were:

- Extend the library, including parameters needed for theoretical calculations up to 200 MeV for energy and non-energy applications.
- Establish well-defined and documented procedures for RIPL maintenance and future updates.
- RIPL validation using large-scale calculations of nuclear reaction across the periodic table (EMPIRE, TALYS, GNASH, UNF) and comparison with the available experimental database (including newest data from HINDAS, nTOF, etc.).
- Uncertainty estimation and/or range of parameter variation for RIPL.
- RIPL to MODLIB interface development (see the MODLIB website http://www.nndc.bnl.gov/nndcscr/model-codes/modlibs/).

The actions to be undertaken prior to the next RCM to be held at the end of 2005 were agreed, together with their relative time-schedule and deadlines (default deadline for all actions is the next RCM if not explicitly stated). The status of the work and the recommendations in regard to RIPL-2/3 contents, expansion of the library and testing are summarized below:

SEGMENT 1: ATOMIC MASSES

(Coordinator: S. Goriely)

The following maintenance actions will be taken:

- Update Audi and Wapstra (2003) compilation.
- Update of the HFB mass and densities tables with the latest available developments.
- The GS-deformation file will be removed.

SEGMENT 2: DISCRETE LEVELS

(Coordinator: R. Capote)

The overall status of the RIPL-2 level segment was considered satisfactory. However the need to establish an automatic update procedure for the Discrete Level segment in the RIPL-3 was stressed, starting from the current ENDSF release. The following maintenance actions will be taken:

- Correct missing information in RIPL-2 tables (Cr-48,V-48,Mn-48,etc) (Koning, Capote).
- Check T. Belgya availability to setup retrieval system directly from ENDSF database (Capote).
- Contact O. Bersillon to find out if he can provide a code to extract level data from ENSDF (Hilaire)

SEGMENT 3: RESONANCES

(Coordinator: M. Herman)

The average resonance parameters of RIPL-2 will be updated within this CRP. The following actions were agreed.

- New evaluation of neutron resonance parameters throughout the periodic table will be performed at BNL and provided by S. Mughabghab.
- New compilation of the proton resonance parameters prepared by S. Sukhoruchkin *et al*. will be analyzed for inclusion within the RIPL-3 database.

SEGMENT 4: LEVEL DENSITIES

(Coordinator: S. Hilaire)

The participants agreed upon the following tasks and their relative deadlines:

- Provide code for K_{vibr} calculations (Plujko, October 2004), including 2+ and 3- collective states systematics.
- Provide total and p-h microscopic LD with normalization/interpolation subroutine (Goriely/Hilaire). Deadline: end of CRP.
- Check MODLIB modules for phenomenological LD calculations as discussed during this meeting (Koning). Agreed to develop codes, allowing for calculation of the total level density including fitting (i.e. input: DISCRETE LEVELS and D_0). If experimental data is not available systematics should be used. It was noted that providing computer codes for LD calculation from the RIPL parameters might be beneficial to the users and would prevent misuse of the library.
- Produce test cases of covariance matrix for LD parameters using KALMANN code (Talou).
- Provide stand-alone version of the Empire-specific NLD subroutine (Herman). Deadline: end of CRP.
- Provide systematic of LD parameters for EMPIRE specific level densities using RIPL 2/3 data (Herman). Deadline: end of CRP.
- Provide file of 2+ states from Nestor & Raman, as well as systematics (Plujko).
- Make available new experimental data on neutron scattering on Si28 and Fe56 nuclei, allowing for a precise estimation of the nuclear level density parameters (Talou).
- Provide Monte Carlo computer code for microscopic single-particle LD calculations (Capote).

SEGMENT 5: OPTICAL MODEL

(Coordinator: A. Koning)

The participants agreed upon the following additional tasks and their relative deadlines (the default deadline is the next RCM if not explicitly stated):

- Development of the optical model potential (OMP) for deformed nuclei. Inclusion of the deformed OMP into RIPL database (Koning). Deadline: end of CRP.

- Provide coupled-channel OMPs for nucleon induced reaction up to 150 MeV for selected fissile nuclei (Talou).
- Develop global OMP for deuteron induced reactions from 1KeV to 200 MeV using Bechetti-Greenless and Koning-Delaroche OMP formulations (Han).
- References to missing EXFOR data for charged particle induced reactions need to be reported to the NDS (October 30, 2004) (Han, Avrigeanu).
- Define how to include double-folding alpha potential within RIPL-3 (Goriely).
- Develop OMPs for alpha induced reactions. Check the behaviour of the alpha OMPs in the low-energy region well below the Coulomb barrier. This energy region is relevant for astrophysical applications (Avrigeanu).
- Extend semi-microscopic OMP for alpha-induced reactions to different mass range (Avrigeanu).
- Evaluate the feasibility of inclusion of the semi-microscopic OMP into the RIPL-3 optical segment (Avrigeanu).
- Encapsulate RIPL-2 interface (om-retrieve.f) in MODLIB format. Evaluate the feasibility of including ECIS code into the same module (Martin).
- Split om-deformation RIPL-2 file into experimental and "theoretical" files (Fukahori).
- Update of the dispersive package included within the RIPL interface (Capote).
- Compilation of new OMP as provided by participants or retrieved from the literature (co-ordinated by Capote).
- Expand RIPL format as needed to accommodate new OMP potentials (Capote).
- Ask INIS for OMP potentials (Capote).
- Ask NSR for OMP potentials (Herman).
- Provide uncertainty or possible range of variation of the OMP parameters (Koning for phenomenological OMP, Hilaire for MOM).

SEGMENT 6: GAMMA-RAY STRENGTH FUNCTIONS

(Coordinator: V. Plujko)

The participants agreed upon the following additional tasks and their relative deadlines:

- Develop a new methodology for treating gamma-ray strength functions with the use of a variational method for centre-of-mass motion extraction (Plujko).
- Compare microscopic temperature dependent gamma-ray strength function with Plujko approach (Plujko, Goriely).
- Compare photo-absorption experimental data from Varlamov *et al.* with RIPL-2 recommendations (Fukahori).
- Check photo-absorption data from the IAEA CRP (see NDS web page).
- Renormalization of the standard MLO1 γ-strength on both GDR data and low-energy $\Gamma\gamma$ data at Sn (Plujko).
- Inclusion of E3 and E4 γ-strength (Check for corresponding references - Talou).
- Implement and test a new methodology for treating gamma-ray strength function in hot nuclei (developed by Plujko for RIPL-3, see GAMMA segment) within EMPIRE system. (Herman).

SEGMENT 7: FISSION

(Coordinator: S. Goriely)

A recent HFB calculation of the potential energy surfaces, including the determination of the fission barrier and barrier width, was presented by Goriely. A comparison of theoretical and experimental n-induced cross sections between 1 to 5 MeV was made and required a renormalization of the fission barrier by more or less 1 MeV, as well as a global modification of the JLMB potential (more precisely, the normalization coefficients were taken as λ_V =0.2 and λ_W =0.3 at all energies).

An accurate determination of the fission cross section would in addition require the determination of the class II states, the band heads, and the use of an adequate coupled-channel neutron potential. For energy applications, the major difficulty today is to describe all existing experimental data within one unique framework. However, when no data is available, it is extremely difficult to predict fission cross section using theoretical calculations. Many parameters are introduced and the resulting predictive power is very weak.

Since a Th-cycle CRP is taking place simultaneously to the present CRP (Capote to check the advance and exact content of the Th-cycle CRP), there is no need to reiterate their work and to concentrate on input parameters for an accurate determination of fission cross section (in particular for energy production). For the same reason, this CRP will not provide a compilation of class-II states. It is proposed that the present CRP will focus on providing global recommendations concerning input parameters (barriers, widths, level densities, potential) to be used when no experimental data exists for fission cross section calculations.

Talou will provide the following information:
- Fission barriers and nuclear level densities for nucleon-induced reactions on selected fissile nuclei.
- Prompt fission neutron information for selected actinides using CEM2k calculations up to 150 MeV.

Goriely will provide (as soon as possible) the following information:
- full 1-dimensional shape barriers calculated within the HFB model.
- inverted parabola fits with barrier heights, widths and saddle point deformations.
- nuclear level densities calculated within the microscopic statistical model based on the single-particle levels at the saddle points deformation for n-induced fission on $^{235\text{-}238}$U, $^{238\text{-}242}$Pu, $^{241\text{-}243}$Am, ^{232}Th and $^{242\text{-}245}$Cm.

GNASH (Talou), TALYS (Koning) and EMPIRE (Herman/Capote) calculations will be carried out to test the fission input on cross section calculation using same and/or different prescriptions for the n-OMP and ground state level density. Blind default calculation of the (n,2n) and (n,f) cross sections will be performed (the coupled-channel neutron potential number 600 of RIPL-2 will be used by default). Modification of input parameters (e.g., neutron potential) will also be done to test to what extent experimental data can be globally reproduced. This sensitivity calculation will not attempt accurate tuning of parameters to reproduce experimental fission cross-section data on actinides of interest to reactor physics. This work will be left to the Th-cycle CRP. Testing of the n-OMP can be done to see to what extend the OMP plays a key role.

Fission fragment distributions have been studied in the "fission product" CRP (Herman will check the content of this CRP) and will not be included in the present CRP.

RIPL-3 RETRIEVAL TOOLS
(Coordinator: T. Fukahori)

Webpage for retrieval of RIPL-3 database will be prepared by Fukahori, based on existing RIPL-2 web interface (http://www-nds.iaea.org/RIPL-2/). The RIPL-1 web-page is available at (http://www-nds.iaea.org/ripl/). Retrieval of the optical model parameters is coupled with optical model code which allows for on-line calculation of elastic angular distributions, total and absorption cross sections, S-matrix elements, and transmission coefficients. The feasibility of using ECIS code for optical model calculations in the RIPL webpage will be studied, allowing for relativistic OMPs to be used.

VALIDATION/TESTING

The following actions were agreed:

- Perform large-scale nuclear data calculations throughout the periodic table using EMPIRE-II system in order to identify energy, target and projectile range in which RIPL-2 input parameters need improvements (Herman).
- Global test of the current RIPL-2 library with the nuclear model code TALYS by dripline to dripline calculations. Assessment of the impact of the RIPL database on the quality of the cross section calculations (Koning).
- Perform large-scale nuclear data calculations throughout the periodic table using EMPIRE-II system to test the new RIPL-3 library (Herman). Deadline: End of CRP.
- Perform global test of the final RIPL-3 library with the nuclear model code TALYS by dripline to dripline calculations (Koning). Deadline: End of CRP.
- Provide comparison between Intranuclear Cascade (INC) and Hauser-Feshbach + preequilibrium calculations in high-energy nucleon induced reactions on selected actinides (Talou).
- Reshaping of a few simple routines for the calculation of basic input data from the nuclear model code WPEC subgroup for RIPL (Koning).
- Validate RIPL-2 Kailas's code for alpha OMP calculations (Avrigeanu, November 2004).
- Testing and upgrade of the RIPL database for radiative strength function calculations in exotic heated nuclei (Plujko).

UNCERTAINTIES

Provide a description of uncertainties affecting the data included in all the different RIPL3 segment, either in a well studied way or in term of general statements.

All coordinators are responsible for providing in a way or another some information regarding the uncertainties affecting the data included in their segment.

UPLOADING NEW FILES

The RIPL-3 area has been set up on the NDS server running under Linux operating system for uploading and downloading new RIPL-3 files. It is accessible (only to the RIPL participants) via ftp to:

```
host name:    amdu1.iaea.org (alias: www-nds.iaea.org)
host ip: 161.5.7.109

username: ripl3
password:   reserved to the RIPL-3 participants
```

The directory structure is the same as the one of RIPL-2:

- ***masses***
- ***levels***
- ***resonances***
- ***optical***
- ***densities***
  - ***total***
  - ***fission***
  - ***partial***
- ***gamma***
- ***fission***

The files should be stored in the appropriate directories. The name of the file should start with the contributor's name followed by additional specification. For example, Plujko's file with GDR parameters should be named as *plujko_gdr.dat*
The directory name should not be repeated (masses, levels, etc.) in the filename. The general structure of the filename should be: [*author-]filename[_specification].dat*
with items within square brackets being optional. Each file must be accompanied by the related file with description. These files should have *.readme* extension instead of *.dat* and should follow the RIPL-2 style.
Related FORTRAN coding for reading the file is recommended for more complicated (non column-oriented) structure.

CONCLUSIONS

Presentations and discussions during the meeting showed good progress of the work for the CRP. Further extensive work needs to be done in the next 15 months so that the necessary progress can be achieved before the next RCM. A truly co-ordinated programme of work was agreed among the participants, leading to several additional actions to be undertaken.

Issues related to level densities, optical model for deformed nuclei, fission barriers and parameter uncertainties were extensively debated. The participants agreed to undertake studies to ensure internal consistency and completeness of the library. The general structure of the RIPL database is well established and will remain the same. The expected output of the CRP is going to be *an updated and expanded RIPL-3 electronic database* based on the

RIPL-2 database. Minor format changes are expected to accommodate additional information needed for non-energy applications.

The main goals to be achieved within the new project were clearly defined, including the maintenance and future update of the RIPL. Emphasis was placed on the determination of parameter uncertainties and validation using large-scale calculations of nuclear reactions across the periodic table. Additional work on RIPL/MODLIB interface development was also recommended.

The proposed features should make RIPL-3 a unique and reliable tool for guiding theoretical calculations at incident energies up to 200 MeV, as needed for modern energy and non-energy applications of nuclear data.

Appendix 1

International Atomic Energy Agency
First Research Coordination Meeting on

"Parameters for Calculation of Nuclear Reactions of Relevance to Non-energy Nuclear Applications"

(RIPL-3)

IAEA Headquarters, Vienna, Austria
23 – 25 June 2004
Meeting Room F 0121

AGENDA

Wednesday 23 June 2004

08:30 - 09:30	Registration (at Gate 1, IAEA Headquarters)
09:30 - 10:00	Opening session
	Welcoming address by A.L. Nichols, Head, NDS Election of chairman and rapporteur Adoption of the Agenda
10:00 - 10:30	Coffee break, Administrative and Financial Matters
10:30 - 12:00	Status Reports:
	S. Goriely M. Avrigeanu V. Plujko R. Capote
12:00 - 13:00	Research Proposals:
	M. Herman H. Yinlu P. Talou
13:00 - 14:00	Lunch
14:00 - 15:00	Research Proposals (cont'd):
	A.J. Koning S. Hilaire T. Fukahori
15:00 - 17:30	Overview and discussion of the RIPL-3 tasks and goals
17:30	Reception

Thursday 24 June 2004

09:00 - 10:30	Optical model segment
10:30 - 11:00	Coffee break
11:00 - 12:30	Level Density segment
12:30 - 14:00	Lunch
14:00 - 17:00	Fission segment
17:00 – 18:00	Masses, Levels and Resonances segments

Friday 25 June 2004

09:00 - 10:00	Gamma Strength Function segment
10:00 - 11:00	Interfaces and retrieval tools
11:00 – 11:30	Coffee break
11:30 - 12:30	Uncertainty estimation of the RIPL parameters
12:30 - 14:00	Lunch
14:00 - 15:00	Interfaces and retrieval tools (cont'd)
15:00 – 17.30	Recommendations for RIPL-3 Drafting of the Summary Report and Formulation of Conclusions
17.30	Review and Approval of the Summary Report Closing of the Meeting

Appendix 2

International Atomic Energy Agency
First Research Coordination Meeting on

"Parameters for Calculation of Nuclear Reactions
of Relevance to Non-energy Nuclear Applications"
(RIPL-3)

IAEA Headquarters, Vienna, Austria
23 – 25 June 2004
Meeting Room F 0121

LIST OF PARTICIPANTS

BELGIUM
Stephane Goriely
Institut d'Astrophysique, CP-226
Campus de la Plaine
Universite Libre de Bruxelles
Boulevard du Triomphe
B-1050 Brussels
Tel: +32 2 650 2843
Fax: +32 2 650 4226
E-mail: sgoriely@astro.ulb.ac.be

CHINA
Han Yinlu
China Institute of Atomic Energy
Nuclear Data Centre
Div. of Nuclear Physics
PO Box 275 (41) Beijing 102413
Tel: +86 10 6935 7275
Fax: +86 10 6935 7008
E-mail: han@iris.ciae.ac.cn

CUBA
Guido Martin Hernandez
Center of Applied Studies for Nuclear
Development, CEADEN-SEAN
Calle 30 e/5ta y 7 ma Miramar, Playa
11300 Ciudad de la Habana
Tel: +537 202 1518
Fax: +537 204 1188
E-mail:guido@ceaden.edu.cu

ROMANIA
Marilena Avrigeanu
Institutul de Fizica si Inginierie Nucleara
"Horia Hulubei"
P.O. Box MG-6
76900 Bucharest
Tel: +40 1 7807040
Fax: +40 1 4231701
E-mail: mavrig@ifin.nipne.ro

UKRAINE
Volodymyr Plujko
Nuclear Physics Department
Faculty of Physics
National Taras Shevchenko University
Prospect Acad. Glushkova 2, Bldg. 11
03022 Kiev-22
Tel: +380 44 258 3494
Fax: +380 44 265 4463
E-mail: plujko@univ.kiev.ua

UNITED STATES OF AMERICA
Patrick Talou
University of California
Los Alamos National Laboratory (LANL)
Theoretical Div.
Group T-16
Los Alamos
Tel: +1 505 667 3821
Fax: +1 505 667 1931
E-mail: talou@lanl.gov

UNITED STATES OF AMERICA
Mike Herman
National Nuclear Data Center
Bldg. 197D
Brookhaven National Laboratory
P.O. Box 5000
Upton, NY 11973-5000
Tel: +1 631 344 2802
Fax: +1 631 344 2806
E-mail: mwherman@bnl.gov

ADVISORS

Commissariat a l'Energie Atomique/DAM
Stephane Hilaire
DPTA/SPN
Ile de France
B.P. No. 12
F-91680 Bruyeres-le-Chatel
France
Tel: +33 1 69264303
Fax: +33 1 69267963
E-mail: stephane.hilaire@cea.fr

Japan Atomic Energy Research Institute
Tokio Fukahori
Nuclear Data Center
Department of Nuclear Energy System
Japan Atomic Energy Research Institute
Tokai-mura, Naka-gun
Ibaraki-ken 319-1195
Japan
Tel: +81 29 282 5907
Fax: +81 29 282 5766
E-mail: fukahori@ndc.tokai.jaeri.go.jp

Nuclear Research and Consultancy Group
Arjan Koning
Building 34.213
Westerduinweg 3
P.O. Box 25
NL-1755 ZG Petten
The Netherlands
Tel: +31 224 564051
Fax: +31 224 568490
E-mail: Koning@nrg-nl.com

OBSERVER
Helmut Leeb
Atominstitut der Österreichischen Universität Wien
AB Kernphysik
Technische Universität Wien
Wiedner Hauptstrasse 8-10
1040 Vienna
Austria
Tel: +43 1 58801-14258
Fax: +43 1 58801-14299
E-mail: leeb@kph.tuwien.ac.at

IAEA PARTICIPANTS:

Roberto Capote Noy
Nuclear Physicist
Nuclear Data Section
Division of Physical and Chemical Sciences
Room A2317
Tel: +43 1 2600 21713
Fax: +43 1 26007
E-mail: R.CapoteNoy@iaea.org

Alan Nichols
Section Head
Nuclear Data Section
Division of Physical and Chemical Sciences
Room A2312
Tel: +43 1 2600-21709
Fax: +43 1 26007
E-mail: A.Nichols@iaea.org

Andrej Trkov
Nuclear Data Physicist
Nuclear Data Section
Division of Physical and Chemical Sciences
Room A2316
Tel: +43 1 2600-21712
Fax: +43 1 26007
E-mail: A.Trkov@iaea.org

Vladimir Pronyaev
Nuclear Data Physicist
Nuclear Data Section
Division of Physical and Chemical Sciences
Room A2320
Tel: +43 1 2600-21717
Fax: +43 1 26007
E-mail: V. Pronyaev@iaea.org

Appendix 3

PRESENTATIONS BY PARTICIPANTS

Appendix 3.1.

Status report: Improvements of microscopic models for practical applications

S. Goriely

Status Report
Improvement of microscopic models for practical applications

S. Goriely
Institut d'Astronomie et d'Astrophysique - Université Libre de Bruxelles

1. Nuclear structure properties
   - HFB Ground State properties (Masses, densities, …)
   - HFB Potential energy surfaces: Fission barriers, width, σ_{nif}
2. E1 γ-ray strength:
   - HFB+QRPA model
3. Nuclear level density:
   - Comparison between microscopic statistical and combinatorial models (cf Segment NLD)

Collaborators: M. Samyn (Brussels), V. Demetriou (Brussels), J.M. Pearson (Montreal), E. Khan (Orsay)

Nuclear structure properties: HFB mass model

Provides all basic ingredients for cross section calculations: masses, deformation, densities, radii, pairing, spl, PES, etc…

Adjustment of a Skyrme force to all (2135) experimental masses within the Hartree-Fock-Bogolyubov approach

Conventional Skyrme force (10 p.) and δ-pairing force (4 p.) to reproduce exp. masses

rms(M) = 650-700 keV on 2135 (Z ? 8) experimental masses (Audi & Wapstra, 2001)
rms(r) = 0.023-0.028 fm on 523 experimental charge radii (Nadjakov et al., 1994)

To be compared with
- Previous HF predictions:
  Traditional Skyrme forces: rms(M) > 2 MeV (120 e-e sph)
- FRDM predictions: rms(M)=676 keV (2135 Z ? 8 nuclei)
  rms(r)=0.045 fm (523 exp. charge radii)

Construction of HFB mass tables

Recent improvements of the HFB mass formulas	Accuracy σ_{rms} (2135 nuc)
HFB-1 masses: M^*_s=1.05, volume pairing	806 keV
HFB-2 masses: M^*_s=1.04, improved pairing descr.	660 keV
HFB-3 masses: M^*_s=1.12, vol+surf pairing (η=α=0.5)	639 keV
HFB-4 masses: M^*_s=0.92, vol. pairing	661 keV
HFB-5 masses: M^*_s=0.92, vol+surf pairing	655 keV
HFB-6 masses: M^*_s=0.80, vol. pairing	666 keV
HFB-7 masses: M^*_s=0.80, vol+surf pairing	658 keV
HFB-8 masses: M^*_s=0.80, vol. pairing, PLN (part.nbr proj.)	641 keV

Complete table of ground-state properties (masses,def,radii,spl,...)
for about 9460 nuclei with 8 ? Z ? 120

HFB calculation of the Fission Barriers
(spontaneous, n-induced and β-delayed fission)

Determination of the potential energy surface within the Constrained HFB model (BSk8)
- introduction of left-right asymmetry with parity projection

Determination of the static fission barriers by the "flooding model"

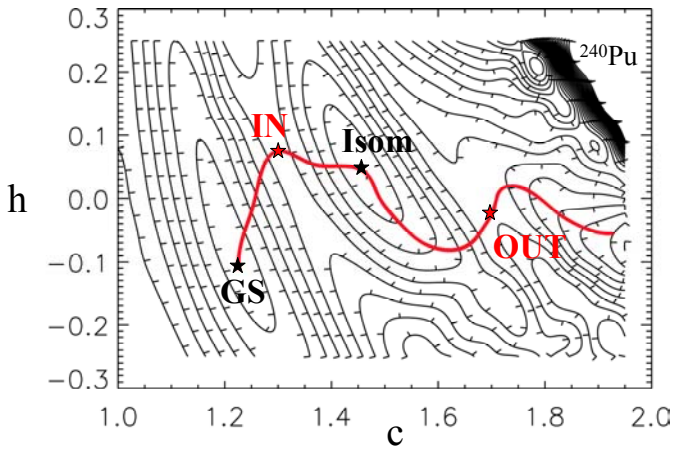

Inner symmetric fission barriers and energy of isomeric states

Exp. Inner barrier

Exp. Energy of Iso.

B_i(HFB) - B_i(Exp)
with BSk8 (HFB+PLN)

E_{iso}(HFB) - E_{iso}(Exp)

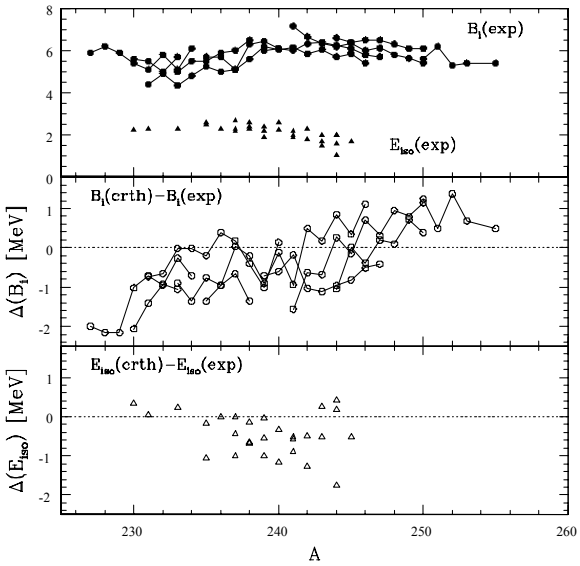

Determination of the fission barrier width

Inverted parabola fits

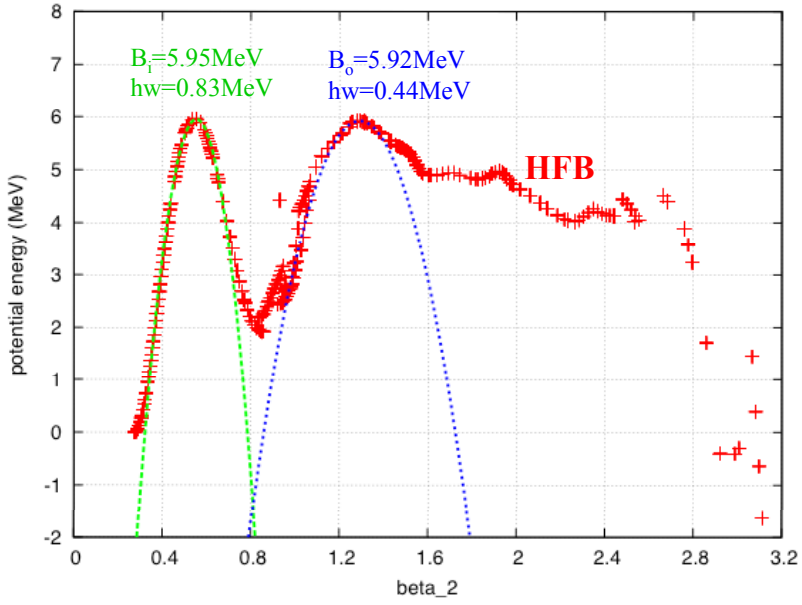

Large scale calculation of fission barriers

- Calculations of the Potential Energy Surfaces (and corresponding fission barriers) for 2300 nuclei with 78?Z?120
- Skyrme force BSk8 within HFB+PLN
- 6 months x 10 CPUs (3Ghz)

Comparison of the n-induced fission cross sections

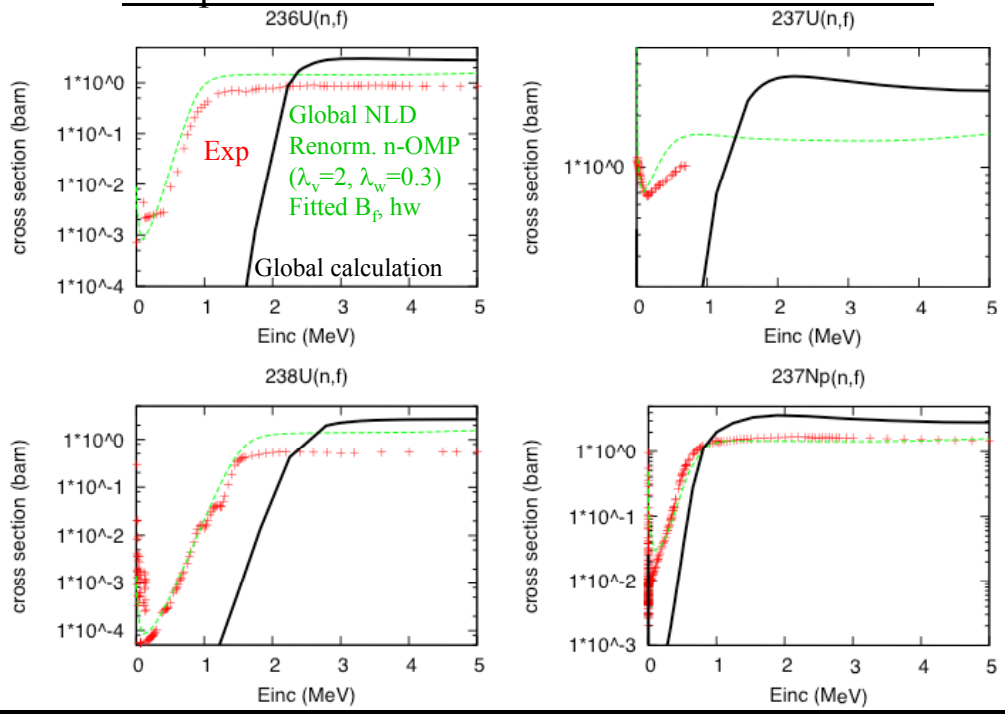

HFB+QRPA γ-ray strength function

1. HFB+ QRPA estimate of the E1-strength distribution based on the Skyrme force (BSk2-BSk7).
   (Skyrme forces derived by a fit on exp. masses)

2. Damping of the collective motions: broadening of the E1-strength distribution based on a folding procedure to reproduce photoabsorption and average resonance capture data.
   (T-dependent correction term)

3. Empirical corrections for deformation effects: splitting of the QRPA strength into two peaks

To appear in Nucl. Phys. A (2004)

Prediction of photoabsorption cross section

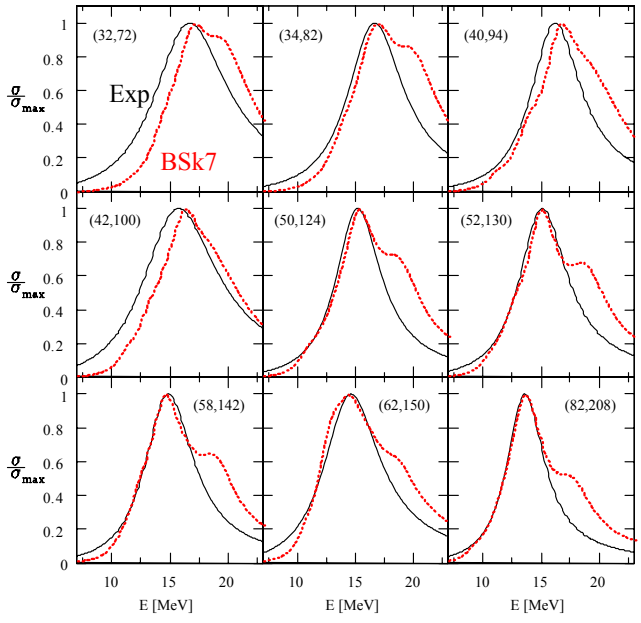

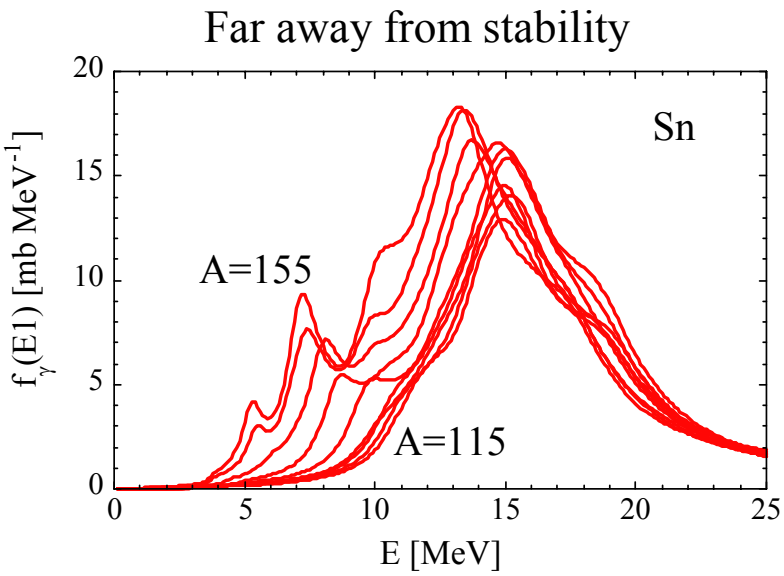

E1 strength calculated within HFB+QRPA for 8300 nuclei with 8?Z?110

To be studied in further details in the HFB framework

- Further analysis of the pairing force (Pairing renormalisation, cut-off prescription, …)
- Double magicity, rotational & vibrational corr., Wigner corr., Coulomb correlation
- Beyond the Skyrme interaction (t_4-term, …)
- Constraints on other physical observables:

Single-particle levels
Giant resonances: GMR, GDR, GQR
Excited states: Nuclear level density
Fission: Fission barriers
Weak interaction: β-strength function

} **TOWARDS UNIVERSALITY**

→ New "improved" force to be used in the estimate of all other ingredients:

- Ground state properties
- Fission barriers
- Nuclear Level Densities (GS & Fission)
- γ-ray strength
- etc…

Improvement of microscopic models for practical applications

S. Goriely
Institut d'Astronomie et d'Astrophysique - Université Libre de Bruxelles

1. Nuclear structure properties
   - HFB Ground State properties (masses, deformations, …)
   - HFB Potential energy surfaces: Fission barriers, width and σ_{nif}
2. E1 γ-ray strength:
   - HFB+QRPA model
3. Nuclear level density:
   - Comparison between microscopic statistical and combinatorial models

Collaborators: M. Samyn (Brussels), V. Demetriou (Brussels), J.M. Pearson (Montreal), E. Khan (Orsay)

Nuclear structure properties: HFB mass model

Adjustement of a Skyrme force to all (2135) experimental masses within the Hartree-Fock-Bogolyubov approach

Conventional Skyrme force (10 p.) and δ-pairing force (4 p.) to reproduce exp. masses

rms(M) = 650-700 keV on 2135 (Z ? 8) experimental masses (Audi & Wapstra, 2001)
rms(r) = 0.023-0.028 fm on 523 experimental charge radii (Nadjakov et al., 1994)

To be compared with
- Previous HF predictions:
  Traditional Skyrme forces: rms(M) > 2 MeV (120 e-e sph)
- FRDM predictions: rms(M)=676 keV (2135 Z ? 8 nuclei)
  rms(r)=0.045 fm (523 exp. charge radii)

Construction of HFB mass tables

Recent improvements of the HFB mass formulas	Accuracy σ_{rms} (2135 nuc)
HFB-1 masses: M^*_s=1.05, volume pairing	**806 keV**
HFB-2 masses: M^*_s=1.04, improved pairing descr.	**660 keV**
HFB-3 masses: M^*_s=1.12, vol+surf pairing (η=α=0.5)	**639 keV**
HFB-4 masses: M^*_s=0.92, vol. pairing	**661 keV**
HFB-5 masses: M^*_s=0.92, vol+surf pairing	**655 keV**
HFB-6 masses: M^*_s=0.80, vol. pairing	**666 keV**
HFB-7 masses: M^*_s=0.80, vol+surf pairing	**658 keV**
HFB-8 masses: M^*_s=0.80, vol. pairing, PLN (part.nbr proj.)	**641 keV**

Complete table of ground-state properties (masses,def,radii,spl,...)
for about 9460 nuclei with 8 ? Z ? 120

Comparison with experimental data

(2135 nuclei: Audi & Wapstra 2001)

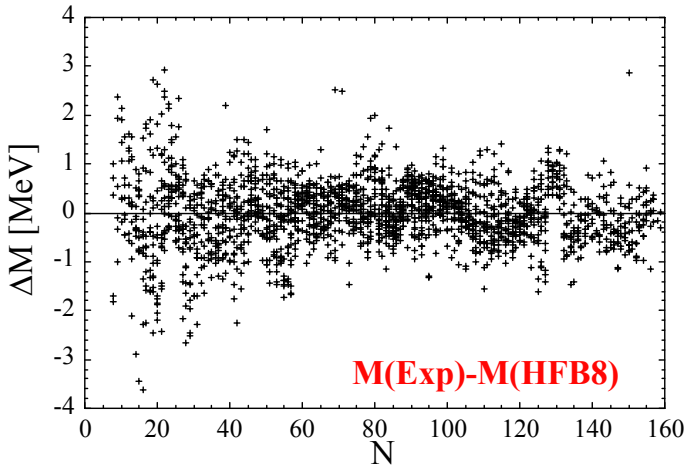

Comparison of the HFB mass predictions

- Global stability of the predictions towards driplines
- Local shell- and pairing-dependent differences

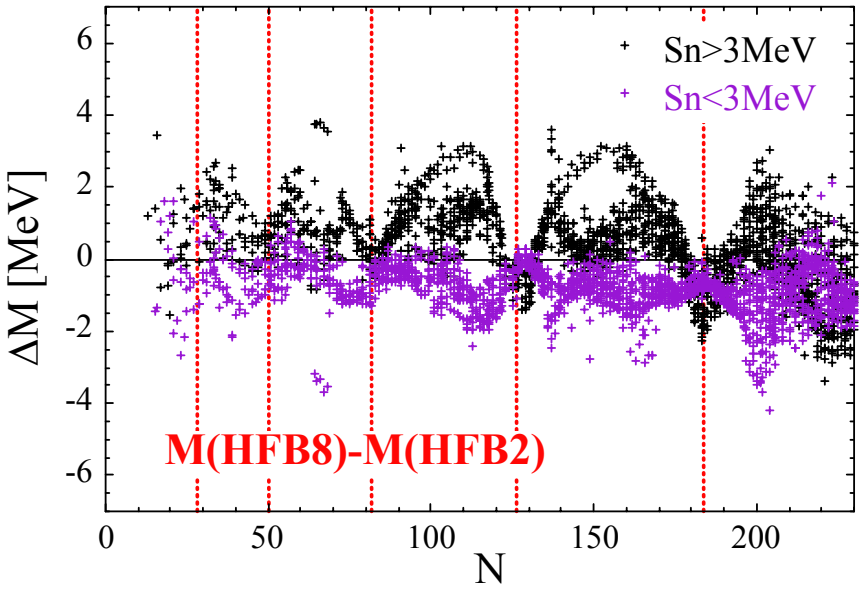

Comparison between HFB and FRDM predictions

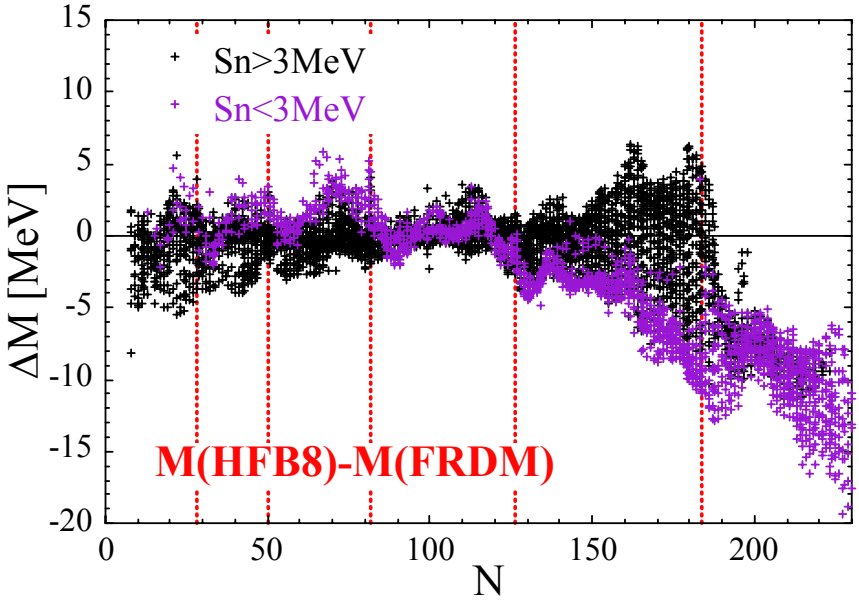

Prediction of charge radii

(523 charge radii: Nadjakov et al. 1994)

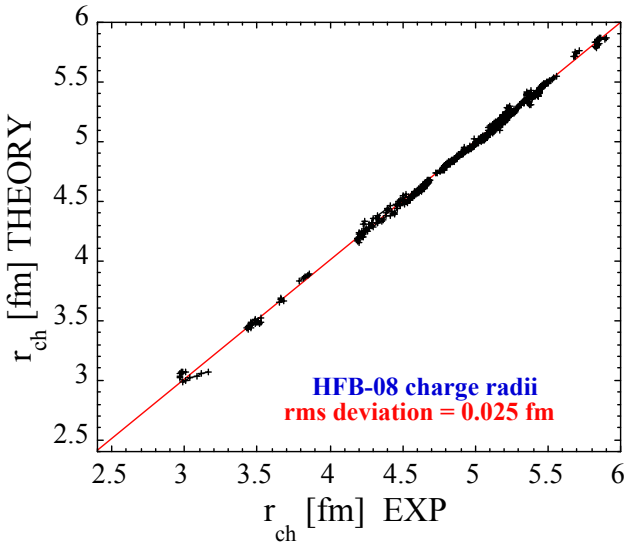

But no kink in the ^{208}Pb isotopic shift

Prediction of charge densities

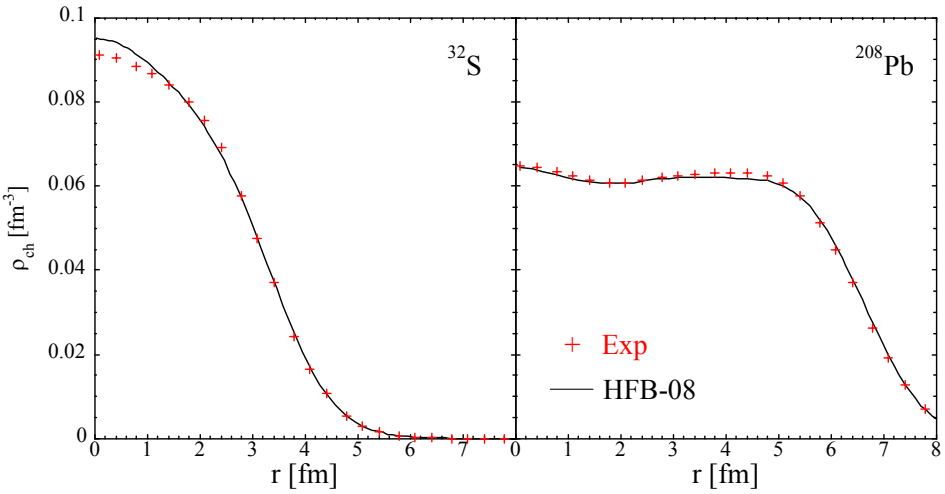

Global predictions of fission barriers

- **Macroscopic-Microscopic Approaches**
  - LDM model (Howard & Moller 1980)
  - TF + FRDM shell corr. (Myers & Swiatecki, 1996)
  - FRLDM (Moller, 2003)
- **Approximation to Microscopic models**
  - ETFSI model (Rayet, Pearson et al. 1995)
- **Mean Field Model**
  - HF-BCS model
  - **HFB model**

HFB calculation of the Fission Barriers
(spontaneous, n-induced and β-delayed fission)

Determination of the potential energy surface within the Constrained HFB model
- introduction of left-right asymmetry with parity projection

Determination of the static fission barriers by the "flooding model"

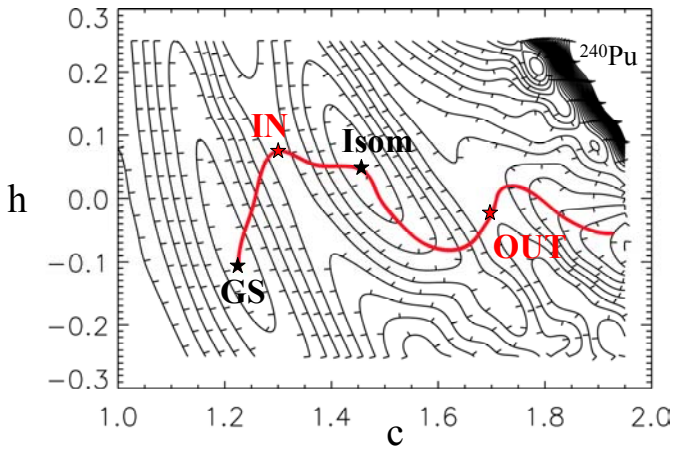

Inner symmetric fission barriers and energy of isomeric states

Exp. Inner barrier

Exp. Energy of Iso.

B_i(HFB) - B_i(Exp)
with BSk8 (HFB+PLN)

E_{iso}(HFB) - E_{iso}(Exp)

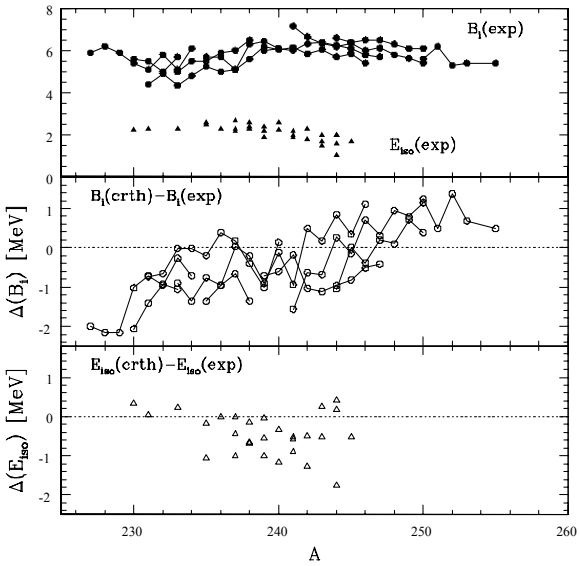

Impact of left-right asymmetry on the outer fission barrier

Symmetric
&
Asymmetric
Outer barriers

$B_o(\alpha=0)$ - $B_o(\alpha>0)$

β_2 at the outer barrier
β_3 at the outer barrier

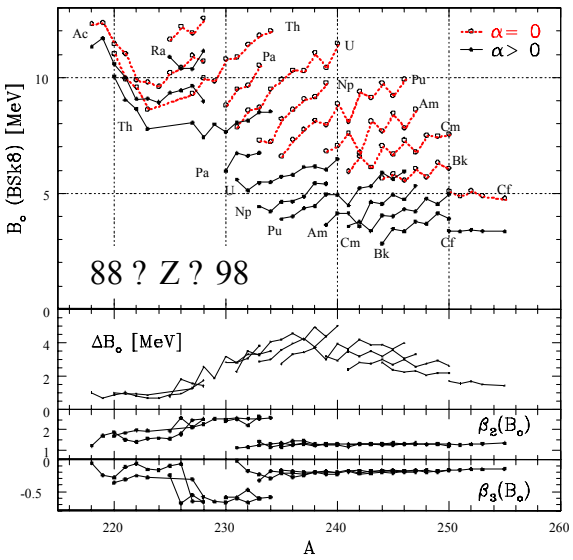

Comparison of outer fission barriers with experimental data

Exp. Fission barriers

B_o(HFB) - B_o(Exp)
with BSk8 (HFB+PLN)

B_o(HFB) - B_o(Exp)
for 2d barrier only

β_2(HFB) at the 2d barrier

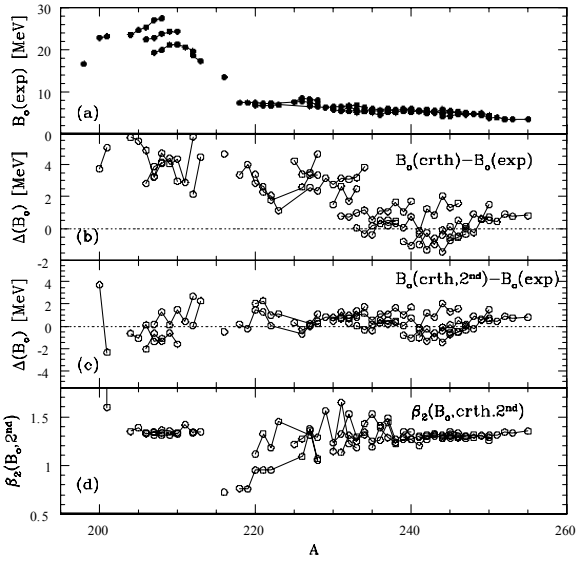

Large scale calculation of fission barriers

- Calculations of the Potential Energy Surfaces and corresponding fission barriers for 2300 nuclei with 78?Z?120
- Skyrme force BSk8 within HFB+PLN
- 6 months x 10 CPUs (3Ghz)

Analysis of the potential energy surfaces

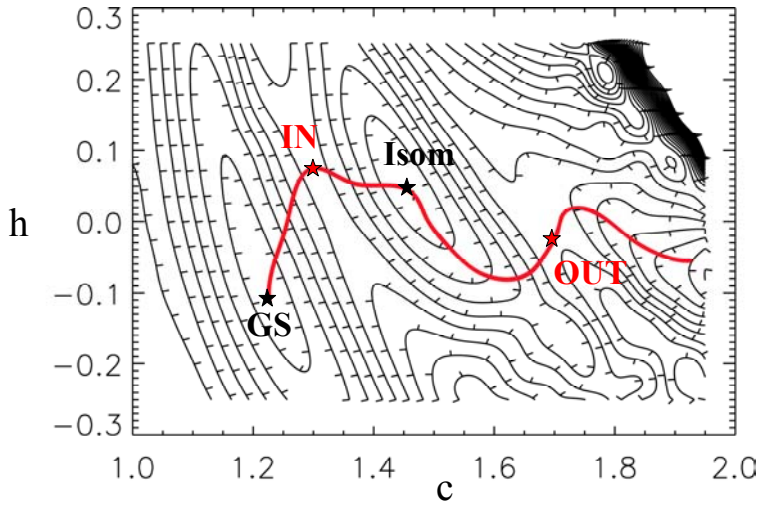

Determination of the fission barrier width

Inverted parabola fits

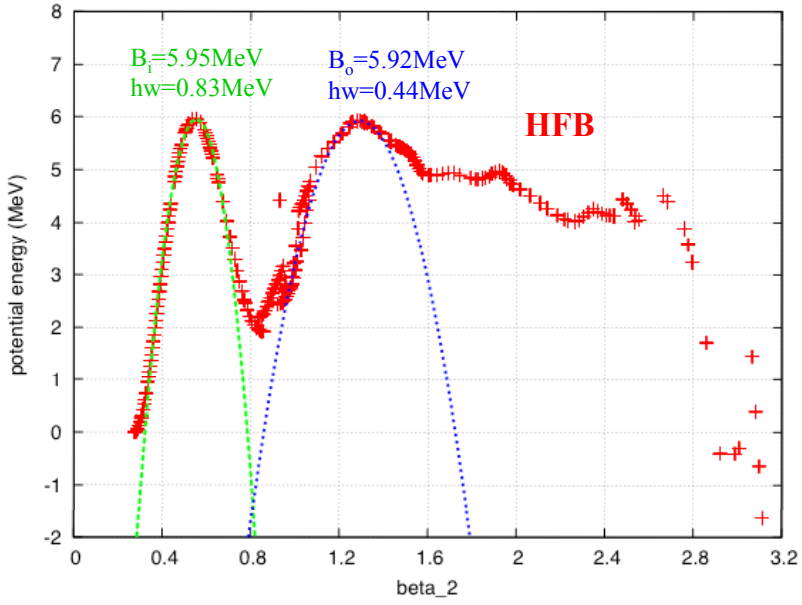

Comparison between Ripl-2 and Bsk-8

		RIPL-2				BSk-8			
nuclide	***Sn***	B_A	hw_A	B_B	hw_B	B_A	hw_A	B_B	hw_B
232Pa	5,55	5	0,6	6,4	0,4	**4,07**	**0,53**	**8,55**	**0,22**
234U	6,84	4,8	0,9	5,5	0,6	**4,78**	**0,74**	**6,63**	**0,3**
235U	5,3	5,25	0,7	6	0,5	**5,05**	**0,8**	**6,57**	**0,34**
236U	6,54	5	0,9	5,67	0,6	**5,4**	**0,8**	**6,77**	**0,4**
237U	5,13	6,4	0,7	6,15	0,5	**5,29**	**0,8**	**7,1**	**0,3**
238U	6,15	6,3	1	5,5	0,6	**5,89**	**0,8**	**7,14**	**0,6**
239U	4,81	6,45	0,7	6	0,5	**5,38**	**0,6**	**7,08**	**0,6**
238Np	5,49	6,5	0,6	5,75	0,4	**5,16**	**0,9**	**6,19**	**0,33**
239Pu	5,65	6,2	0,7	5,7	0,5	**5,3**	**0,98**	**5,77**	**0,64**
240Pu	6,53	6,05	0,9	5,15	0,6	**5,95**	**0,8**	**5,92**	**0,44**
241Pu	5,24	6,15	0,7	5,5	0,5	**5,22**	**0,87**	**5,39**	**0,5**
242Pu	6,31	5,85	0,9	5,05	0,6	**6,35**	**0,96**	**6,27**	**0,32**
243Pu	5,03	6,05	0,7	5,45	0,5	**6,24**	**0,85**	**6,28**	**0,4**
245Pu	4,77	5,85	0,7	5,25	0,5	**6,22**	**0,8**	**6,59**	**0,4**
244Am	5,37	6,25	0,7	5,9	0,53	**6,02**	**0,8**	**5,37**	**0,4**
244Cm	6,8	6,18	0,9	5,1	0,6	**6,45**	**0,98**	**5**	**0,34**
246Cm	6,46	6	0,9	4,8	0,6	**6,7**	**0,9**	**5,15**	**0,33**
247Cm	5,16	6,12	0,7	5,1	0,5	**6,42**	**0,9**	**5,02**	**0,33**
248Cm	6,21	5,8	0,9	4,8	0,6	**6,7**	**0,7**	**5,75**	**0,5**
249Cm	4,71	5,63	0,7	4,95	0,5	**6,38**	**0,6**	**5,46**	**0,34**

Determination of the n-induced fission cross section

Fission transmission coefficients

Hill-Wheeler formula: single- or double-humped barrier

$$T(E,J,\pi) = ?\rho(e,J,\pi)\, T_{HW}(\Delta,h\omega)\, d\varepsilon \quad \text{with}$$

$$T_{HW}(E,h\omega)=[1+\exp(-2\pi E/h\omega)]^{-1} \text{ and } \Delta=E-B_f-\varepsilon$$

+ Sub-barrier effects (picket fence model)

- Fission barriers and width from HFB (BSk8) calculation
  - allowed adjustment of B_f ±1MeV
- Global nuclear level densities
  - same input as for the GS (preferably no pairing)
- JLM-B n-OMP
  - possibly renormalized: λ_v=2; λ_w=0.3 for strongly deformed nuclei

Nuclear Level Density at Saddle Points

- Fission Barriers and saddle point deformations (c,h,α) determined within ETFSI method for 2300 (78 ? Z ? 120) nuclei
- Nuclear properties (spl, pairing) at the inner and outer saddle points with constrained HF-BCS model (MSk7 Skyrme force constrained on Q,O,H)
- NLD in the framework of the microscopic statistical model based on HF-BCS spl predictions at saddle points
  - no damping of collective effects
  - (constant-G pairing with the same strength as in GS)
  - rotational enhancement
  - Double level density for l-r asymmetric barriers

→ **NLD in a table format at inner and outer saddle points for 2300 nuclei**

Comparison of the n-induced fission cross sections

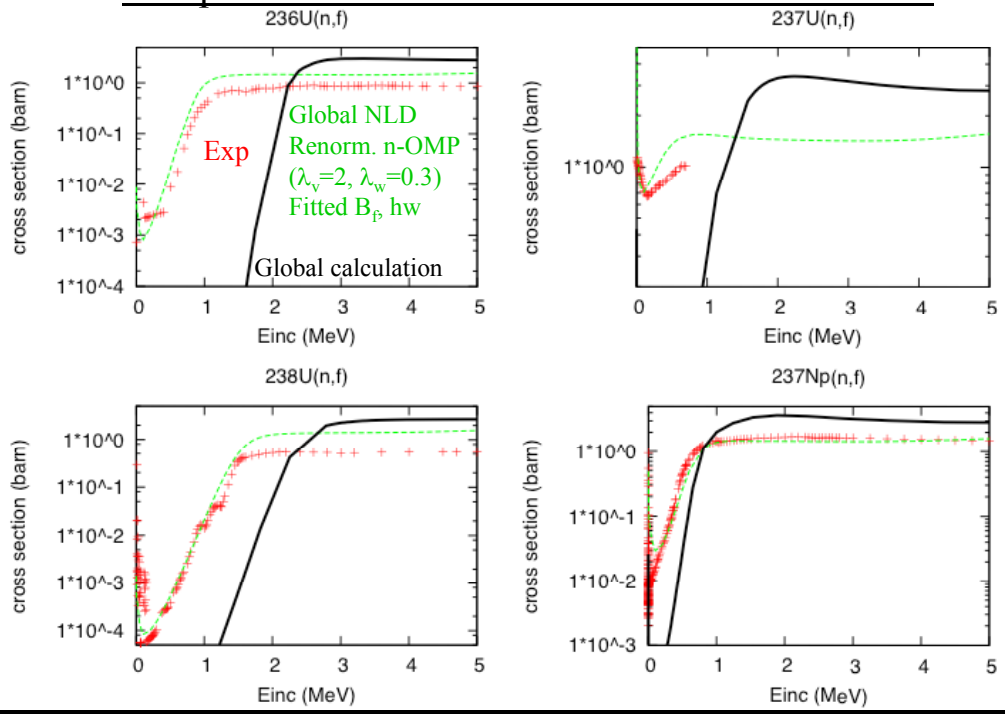

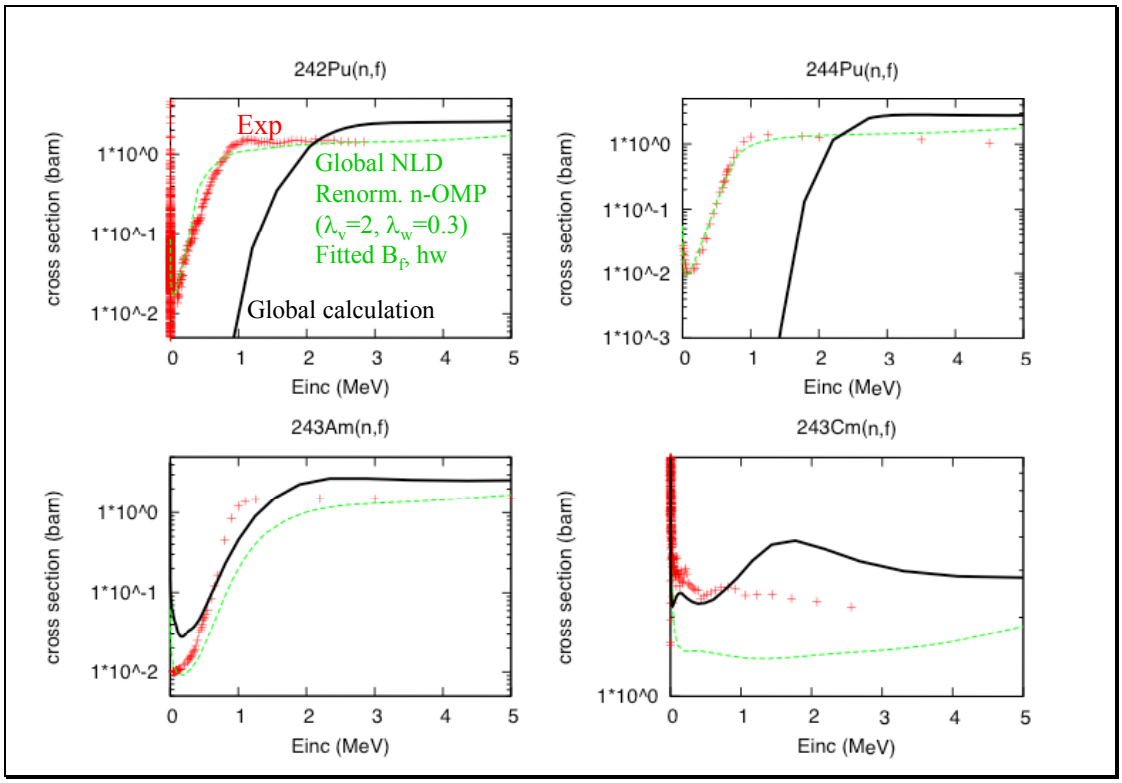
242Pu(n,f)
Exp
Global NLD
Renorm. n-OMP
(λv=2, λw=0.3)
Fitted Bf, hw
Global calculation
244Pu(n,f)
243Am(n,f)
243Cm(n,f)
cross section (bam)
Einc (MeV)
1*10^0
1*10^-1
1*10^-2
1*10^-3

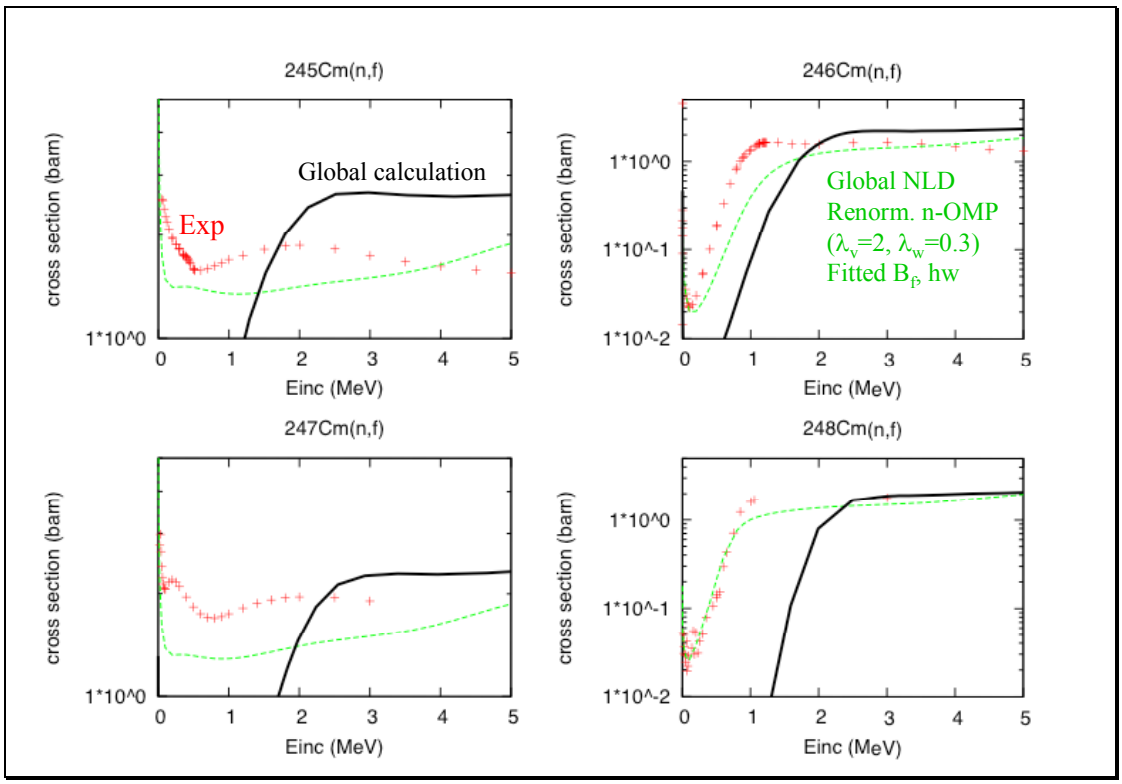
245Cm(n,f)
Global calculation
Exp
246Cm(n,f)
Global NLD
Renorm. n-OMP
(λv=2, λw=0.3)
Fitted Bf, hw
247Cm(n,f)
248Cm(n,f)
cross section (bam)
Einc (MeV)
1*10^0
1*10^-1
1*10^-2

HFB+QRPA γ-ray strength function

1. HFB+ QRPA estimate of the E1-strength distribution based on the Skyrme force (BSk2-BSk7).
   (Skyrme forces derived by a fit on exp. masses)

2. Damping of the collective motions: broadening of the E1-strength distribution based on a folding procedure to reproduce photoabsorption and average resonance capture data.
   (T-dependent correction term)

3. Empirical corrections for deformation effects: splitting of the QRPA strength into two peaks

To appear in Nucl. Phys. A (2004)

Prediction of photoabsorption cross section

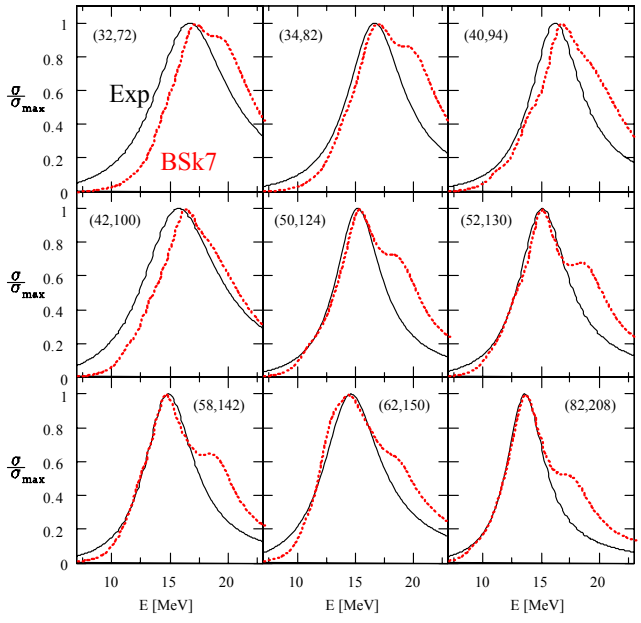

Prediction of E1 strength function

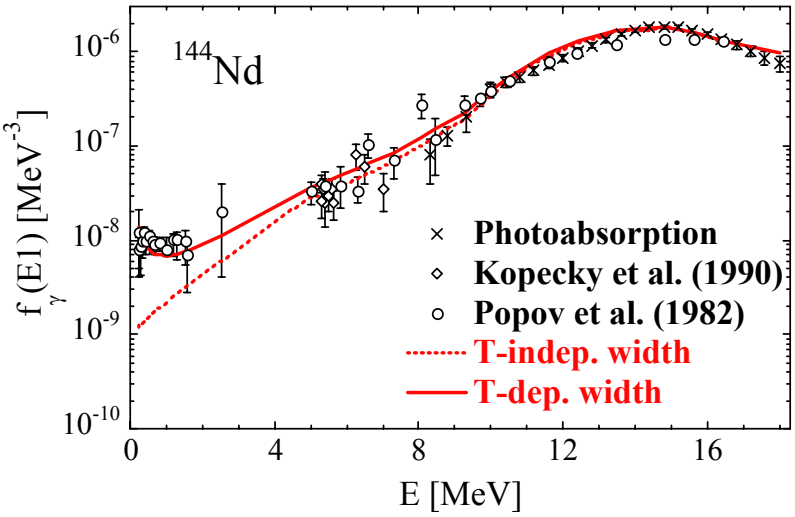

Prediction of E1 strength function

Resolved-resonance and thermal capture measurements, RIPL2 (2004)

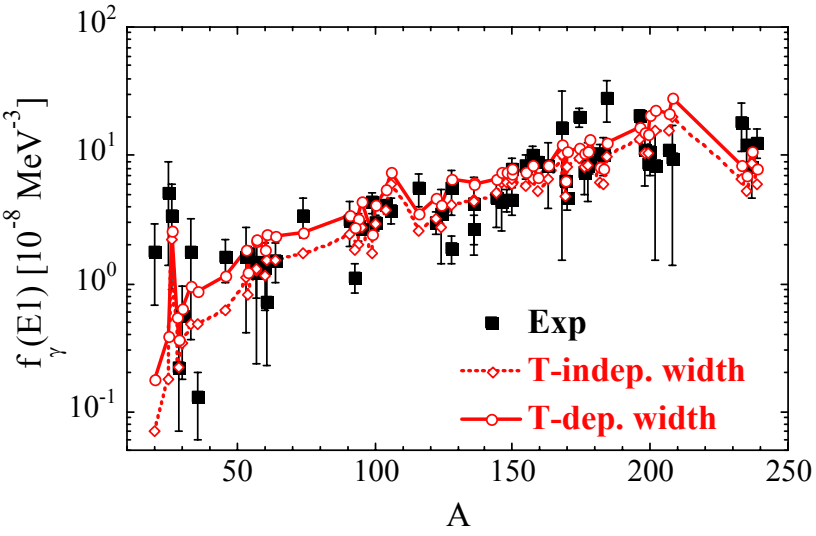

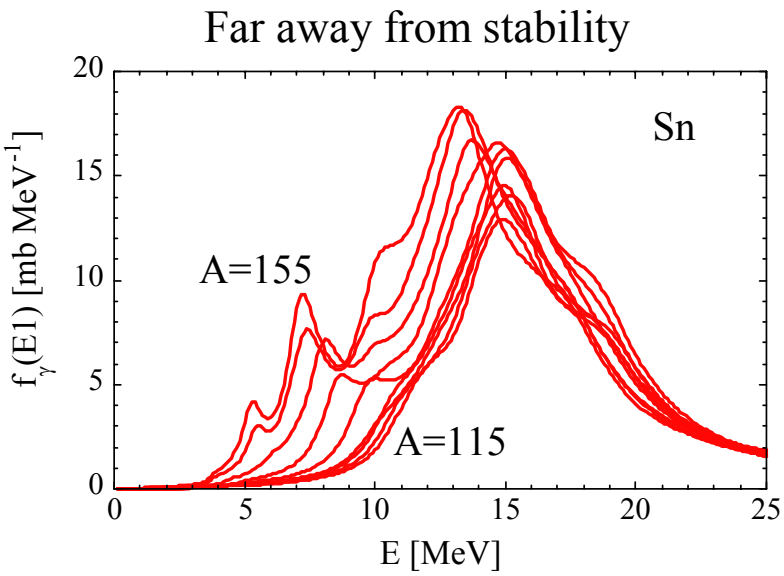

E1 strength calculated within HFB+QRPA available for 8300 nuclei with 8?Z?110

To be studied in further details in the HFB framework

- Further analysis of the pairing force (Pairing renormalisation, cut-off prescription, …)
- Double magicity, rotational & vibrational corr., Wigner corr., Coulomb correlation
- Beyond the Skyrme interaction (t_4-term, …)
- Constraints on other physical observables:

Single-particle levels
Giant resonances: GMR, GDR, GQR
Excited states: Nuclear level density
Fission: Fission barriers
Weak interaction: β-strength function

} **TOWARDS UNIVERSALITY**

→ New "improved" force to be used in the estimate of all other ingredients:

- Ground state properties
- Fission barriers
- Nuclear Level Densities (GS & Fission)
- γ-ray strength
- etc…

A global microscopic NLD formula

- NLD formula within the statistical (partition function) method based on the HF-BCS (MSk7) ground-state properties
  - Single particle level scheme
  - Ground-state deformation parameters and energy
  - Pairing strength (though renormalized consistently)
- Microscopic NLD formula includes
  - Shell correction inherent in the mean field s.p. level scheme
  - Pairing correction (in the constant-G approximation) with blocking effects
  - Spin-dependence with microscopic shell and pairing effects
  - Deformation effects included in
    - the single-particle level scheme
    - the collective contribution of the rotational band on top of each intrinsic state
    - disappearance of deformation effects at increasing excitation energies

→ **Reliability**: Exact solution the analytical formulas tries to mimic
→ **Accuracy**: Competitive with parametrized formulas in reproducing experimental data

Comparison with experimental neutron resonance spacings

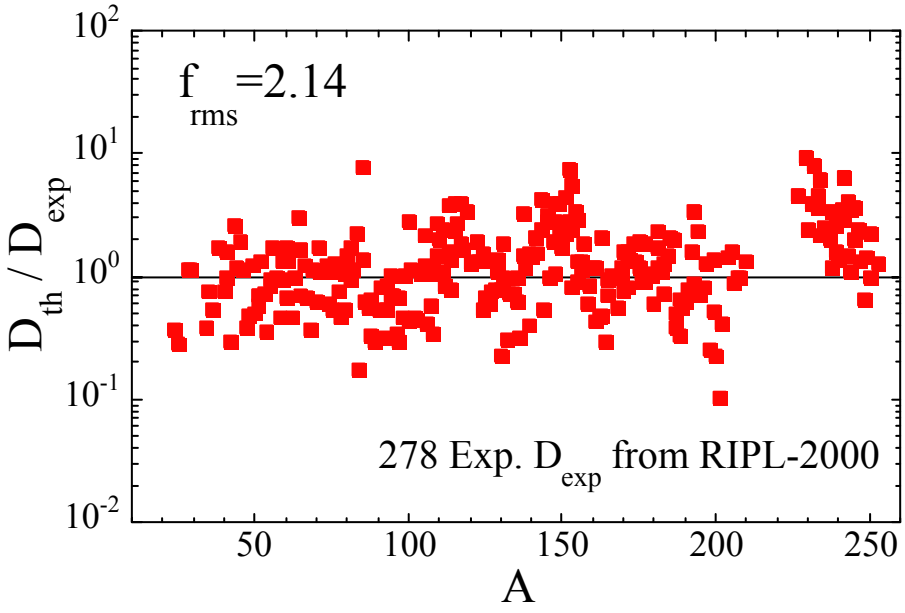

Comparison with experimental low-lying states

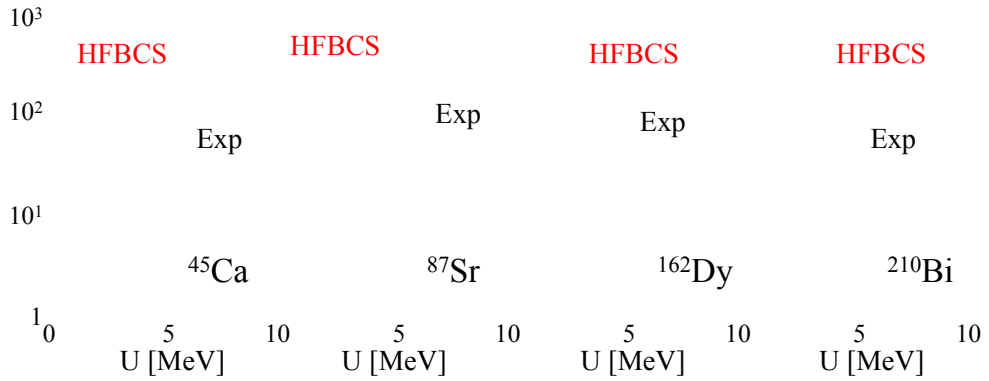

Renormalization on experimental data

- s-wave resonance spacings for 278 nuclei
- spectra of low-lying states for 1026 nuclei

Determination of N_{max} (Nbr of levels up to which the level scheme is complete)

Traditionally determined with Cst-T formula (independently of NLD)

Comparison of NLD predictions

Microscopic NLD formula based on HF-BCS

vs

Analytical shell-corrected Back-Shifted Fermi Gas

U=50 MeV

A global combinatorial microscopic NLD formula

Hilaire (2003)

- Ground-state properties obtained within HFB with the BSk7 Skyrme force (force fitted to 2135 exp. nuclear masses with σ=0.658MeV)
  - Single particle level scheme
  - Pairing strength
- NLD formula within the combinatorial method (Hilaire 2003)
  - Parity, angular momentum, pairing correlations treated explicitely
  - Inclusion of a simple approximation of the
    - Vibrational enhancement (cf Ripl-1)
    - Rotational enhancement (σ^2_{perp})
    - Disappearance of deformation effects at increasing excitation energies

Comparison with experimental neutron resonance spacings

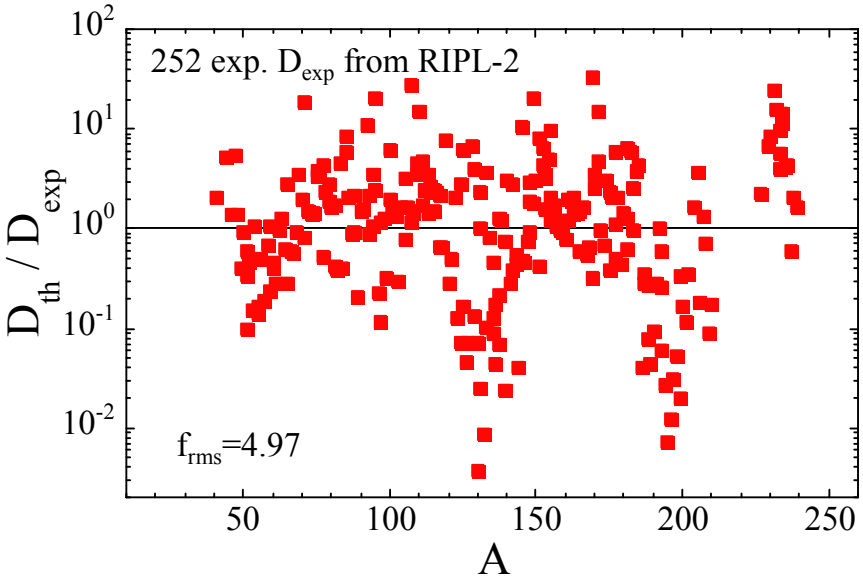

Very promising …

Comparison of NLD predictions

Microscopic Statistical NLD formula based on HF-BCS
vs
Microscopic Combinatorial NLD based on HFB

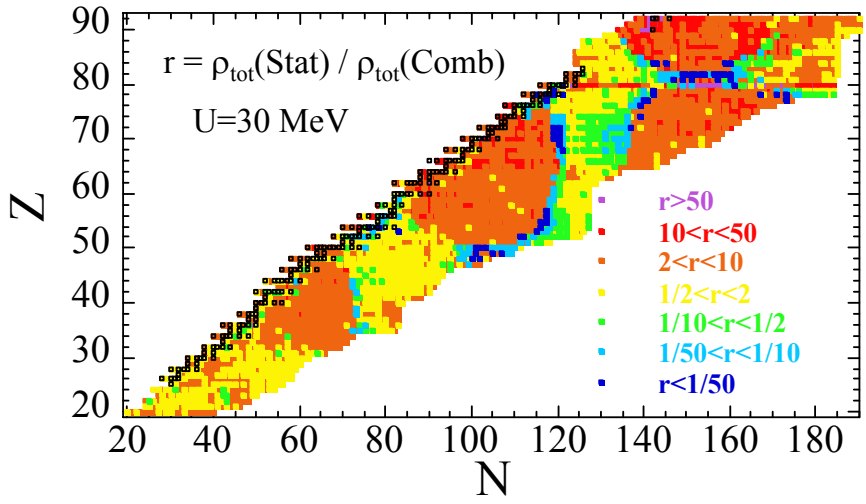

Impact of the single-particle basis on deformed configuration

QuickTime™ and a TIFF (LZW) decompressor are needed to see this picture.

QuickTime™ and a TIFF (LZW) decompressor are needed to see this picture.

But should ρ_{sph} be determined with the spherical spl scheme ?

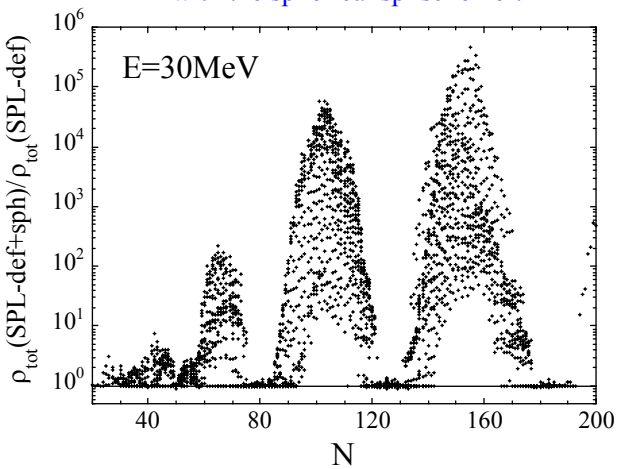

Comparison of NLD predictions

Microscopic Statistical NLD formula based on HF-BCS
vs
Microscopic Combinatorial NLD based on HFB

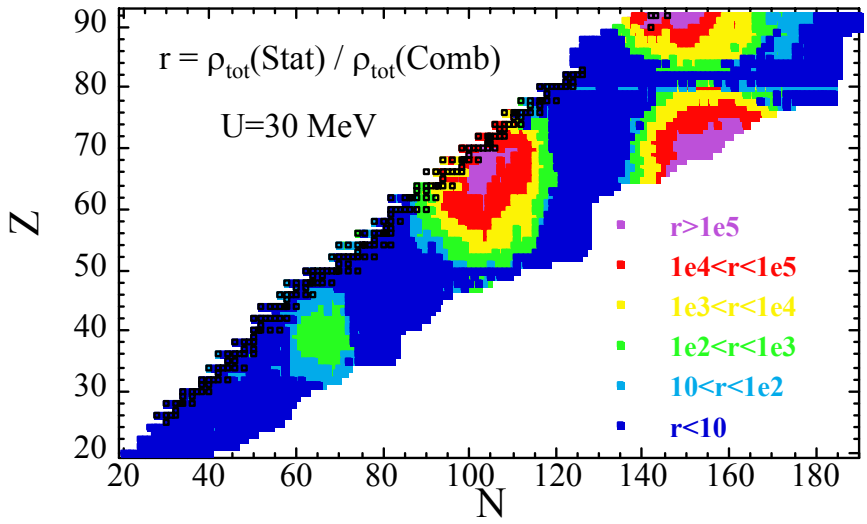

Nuclear structure properties: HFB mass model

Adjustement of a Skyrme force to all (2135) experimental masses within the Hartree-Fock-Bogolyubov approach

$$E_{HFB} = E_{sph} + E_{def} + E_{wig}$$

Conventional Skyrme force (10 p.)

QuickTime™ and a
TIFF (LZW) decompressor
are needed to see this picture.

Density-(in)dependent staggered δ-pairing force:
- stronger proton than neutron pairing
- stronger odd- than even-nucleon pairing

QuickTime™ and a
TIFF (LZW) decompressor
are needed to see this picture.

Single-particle levels in ^{16}O, ^{132}Sn and ^{208}Pb

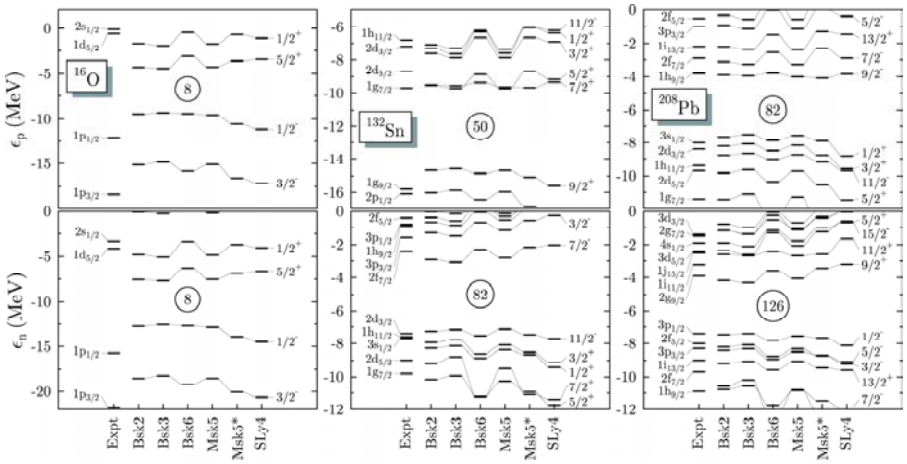

Shell effects far away from the valley of β-stability

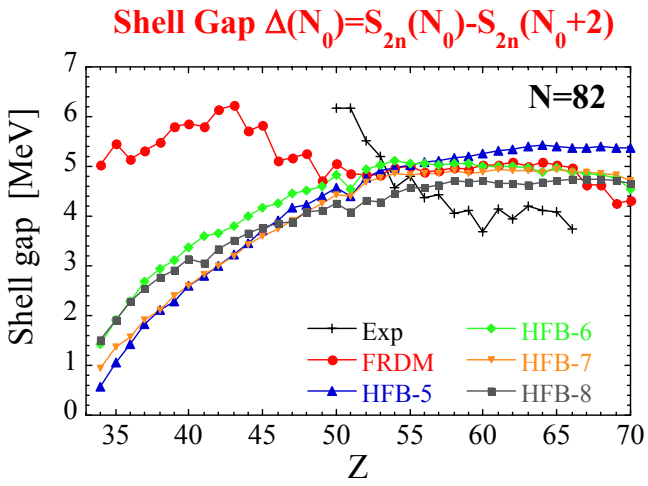

Giant Quadrupole Resonance within HFB+QRPA

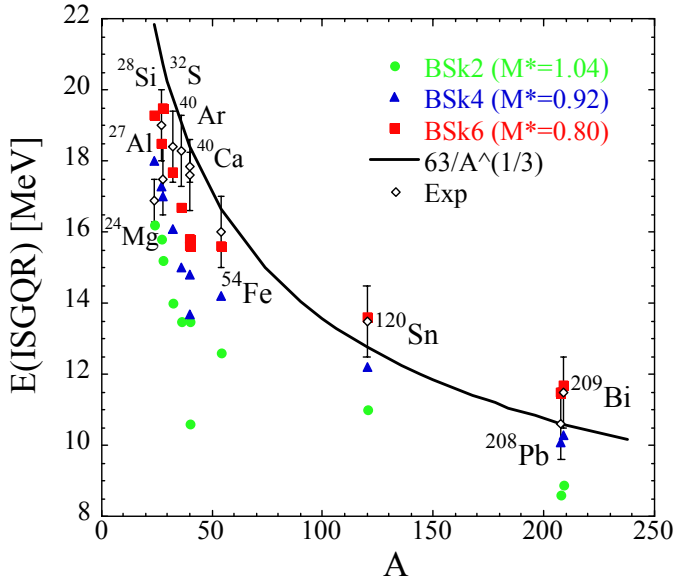

Appendix 3.2.

Microscopic optical potential for low energy α-particles interacting with A~100 target nuclei

M. Avrigeanu, M. von Oertzen and V. Avrigeanu

Microscopic optical potential for low energy α-particles interacting with A~100 target nuclei

M. Avrigeanu[1], W. von Oertzen[2], and V. Avrigeanu[1]

[1]*Association EURATOM-NASTI, IFIN-HH, Bucharest, Romania*
[2]*Freie Universitat Berlin, Fachbereich Physik, and HMI, Berlin, Germany*

Contents

- **MOTIVATION**: (n,xα) → structural-material radiation damage effects
- **APPROACH:**
- **(I) DOUBLE-FOLDING** (DF) real potential
- **(II) Phenomenological W(E)** below 35 MeV
- **(III)** Real DF **+** W(E) **+ DISPERSION RELATIONS**
- **(IV) Phenomenological OMP** below 35 MeV (E-dependent)
  [Nucl. Phys. **A723**, 104 (2003)]
- **(V) DF-equivalent** phenomenological OMP below 35 MeV

- **OPEN QUESTIONS**:
  - α-nucleus **phenomenological OMP - still extensively used**
  - **no global OMP** for α-particles[1] that
    - fit scattering from **many nuclei**
    - over **wide range of energies**
    - with **good accuracy**
  - **uncertainties of parameter sets** critically depend on:
    - particular α-nucleus system
    - the incident energy
    - precision of analyzed data

[1] **RIPL, Report IAEA-TECDOC-1034, IAEA, Vienna, 1998; http://www-nds.iaea.or.at/ripl/**

Microscopic Real Optical Potential

$$U(E,\mathbf{R}) = \int d\mathbf{r}_1 \int d\mathbf{r}_2 \; \rho_1(r_1)\, \rho_2(r_2)\, v_{eff}(E, \mathbf{s}=\mathbf{R}+\mathbf{r}_1-\mathbf{r}_2)$$

- $\rho_{1,2}$ - density distributions of projectile (1) and target (2) nuclei
- $\mathbf{v_{eff}}$ - effective **NN**-interaction:
  isoscalar and isovector components of
  direct and exchange parts of M3Y interaction
  (**g**-matrix calculations using Reid/Paris[1] **NN** potential)

[1] G. Bertsch *et al.*, Nucl. Phys. A284, 399 (1977)
N. Anantaraman *et al.*, Nucl.Phys. A398, 269 (1983)

Approximations

- DME-leading term (Negele-Vautherin'72)

  $\rho(\mathbf{R},\mathbf{R}+\mathbf{s}) = \rho(\mathbf{R}+\mathbf{s}/2) J_1[k_F(\mathbf{R}+\mathbf{s}/2)s]$

- Campi-Bouyssy'78 for average relative momentum, $\mathbf{k_F=k_{av}}$

  $k_{av}(r) = 5/(3\rho(r))[\tau(r)-(1/4)\nabla^2\rho(r)]^{1/2}$

- Kinetic-Energy Density (τ: **MTF**-Krivine-Treiner'79)

  $\tau(\rho) = \alpha\rho(r)^{5/3} + \beta(\nabla\rho)^2/\rho$

- The frozen-density approximation (Satchler'79, Khoa'94)

  $F(\rho) = F[\rho_1(\mathbf{r}_1+\mathbf{s}/2)+\rho_2(\mathbf{r}_2-\mathbf{s}/2)]$.

(I) DOUBLE-FOLDING (DF) real potential

- **Basic DF input**:
  - ❖ nuclear densities of the colliding nuclei (Fig.1)
    - ➢ Baye density[1]
    - ➢ experimental Tanihata densities[2]
    - ➢ realistic densities of cluster-orbital shell model approximation[3] (COSMA)
  - ❖ effective nucleon-nucleon (NN) interaction:
    - ➢ energy- and density-dependent (DDM3Y/BDM3Y) Paris and Reid
    - ➢ explicit treatment of the exchange potential[4,5]
- **Validation** *(no adjustable parameter or normalization constant)*:
  - ♦ comparison with phenomenological[6] OPs
  - ♦ description of (α,α_0) angular-distribution systematics (Fig. 2) and (Fig. 3)

[1] D. Baye et al., Phys. Rev. C 54, 2563 (1996)
[2]] I. Tanihata et al., Phys. Lett. B 289, 261 (1992).
[3] M.V. Zhukov et al. Phys Rep. 231, 151 (1993).
[4]] Dao T. Khoa, Phys. Rev. C 63, 034007 (2001).
[5] M. Avrigeanu et al., Phys. Rev. C 62, 017001 (2000); Nucl. Phys. A693, 616 (2001).
[6] L.W. Put and A.M.J. Paans, Nucl. Phys. A291, 93 (1977); L.McFadden and G.R. Satchler, Nucl. Phys. A84, 177 (1966); M. Nolte et al., Phys. Rev. C 36, 1312 (1987); V. Avrigeanu et al., Phys. Rev. C 49, 2136 (1994).

Alpha-particle density distributions

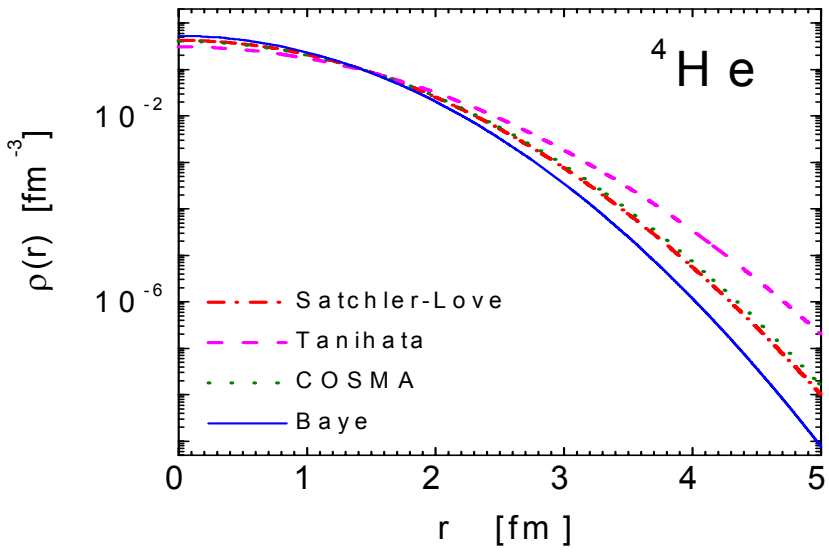

α+α scattering
at incident energies below the inelastic threshold

($E_{threshold}$=17.25 MeV)

- **No need** of the **imaginary** optical potential
- **Test for ingredients** of the microscopic real potential:
  - **density distribution** of α-particle
  - **effective NN-interaction**
- Experimental systematics best description provided by:
  - **Baye-density** for α-particle
  - **M3Y-Reid** effective **NN** - interaction

Comparison between alpha-particle density distributions

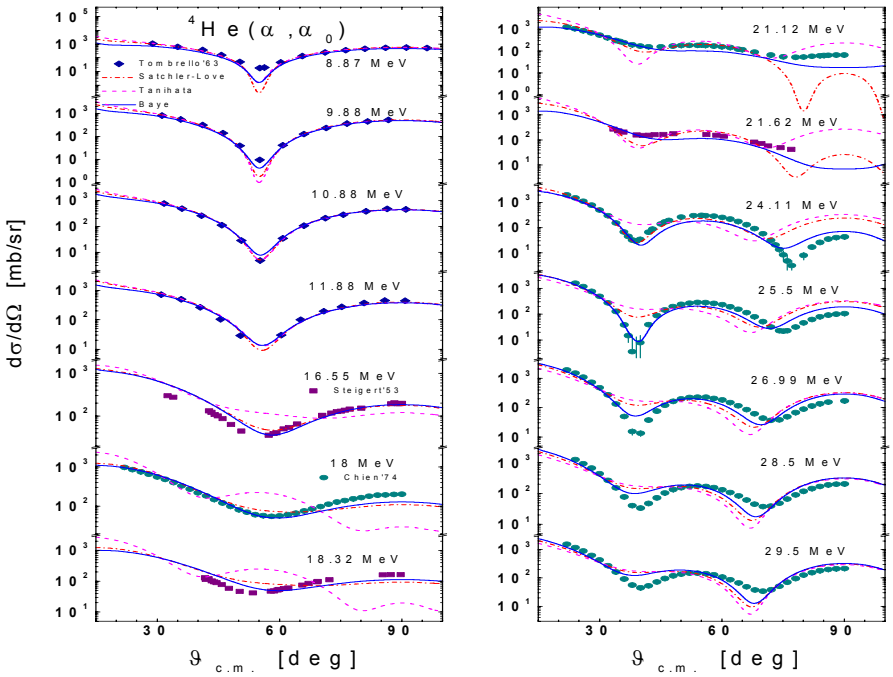

Comparison between M3Y Reid/Paris effective interactions

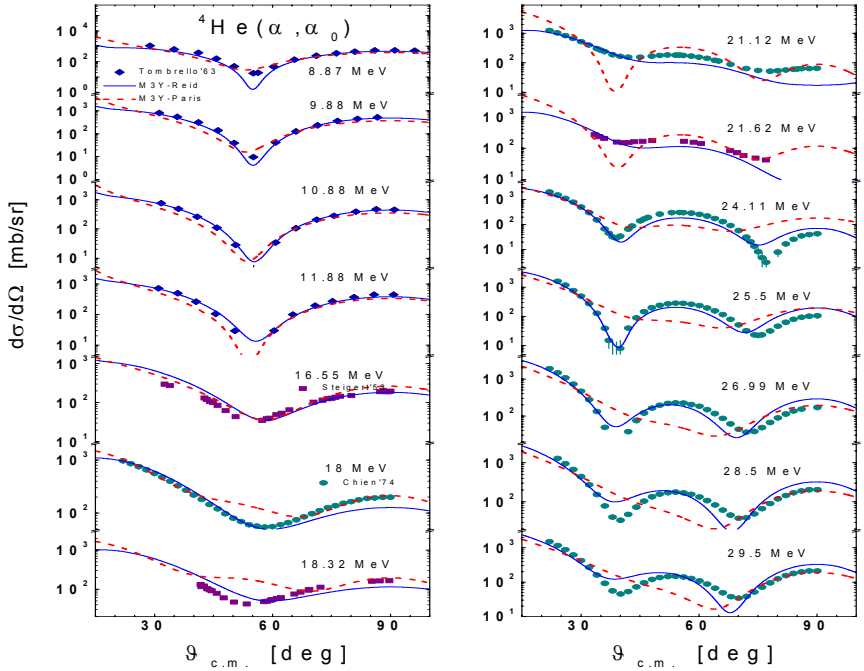

- **(II) Phenomenological OMP below 40 MeV (E-dependent)**

  - (α,α_0) **angular-distribution systematics:**

    ❖**strong energy dependence at 'low energies'[1]: 13 - 32 MeV** (Figs. 5,6):

    ^{90}Zr, ^{107}Ag: 15 MeV
    ^{92}Mo: 13.8, 16.4, 19.5 MeV
    ^{89}Y, ^{90,91}Zr: 21, 23.4, 25 MeV
    ^{94}Mo, ^{107}Ag, ^{116,122,124}Sn: 25.2 MeV
    ^{92,94,96,98,100}Mo: 32.2 MeV

  - **energy-dependent parameters** compared with individual values[1] for **dispersive correction** (Fig. 7)

[1] **L.W. Put and A.M.J. Paans, Nucl. Phys. A291, 93 (1977); M. Wit et al., Phys. Rev. C 12, 1447 (1975); S.J. Burger and G. Heymann, Nucl.Phys. A243, 461 (1975); O.V. Bespalova et al., Yad. Phys. 56, 113 (1992); Zs. Fulop et al. ,Phys. Rev. c 64, 065805 (2001).**

Dispersion correction (Mahaux, Ngo, Satchler'86)

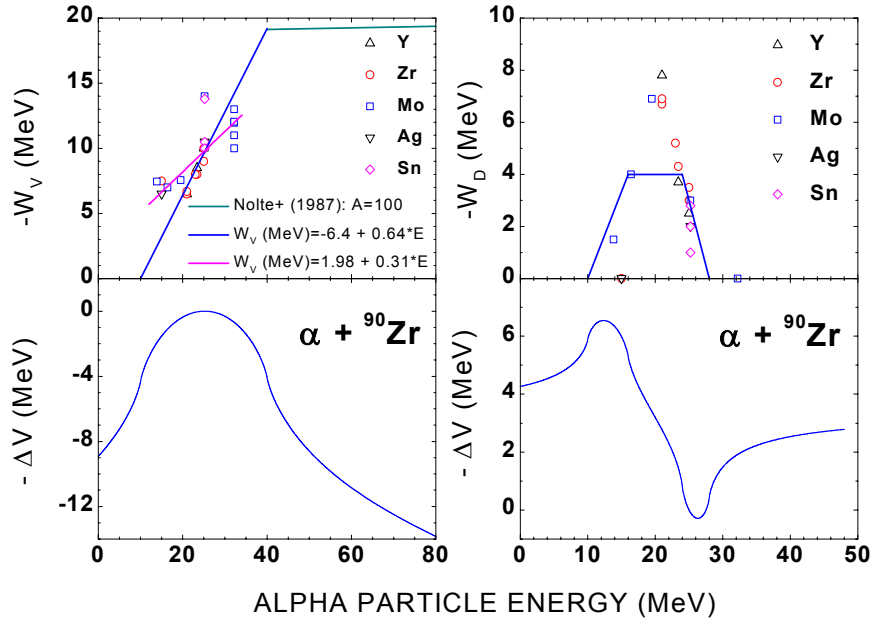

DF-real & phenomenological imaginary potential

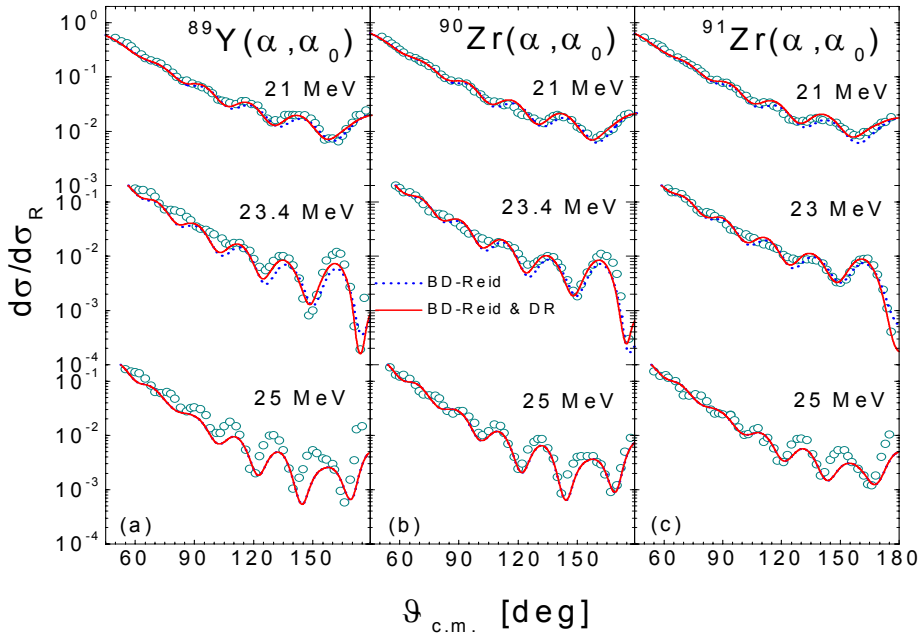

DF-real & phenomenological imaginary potential

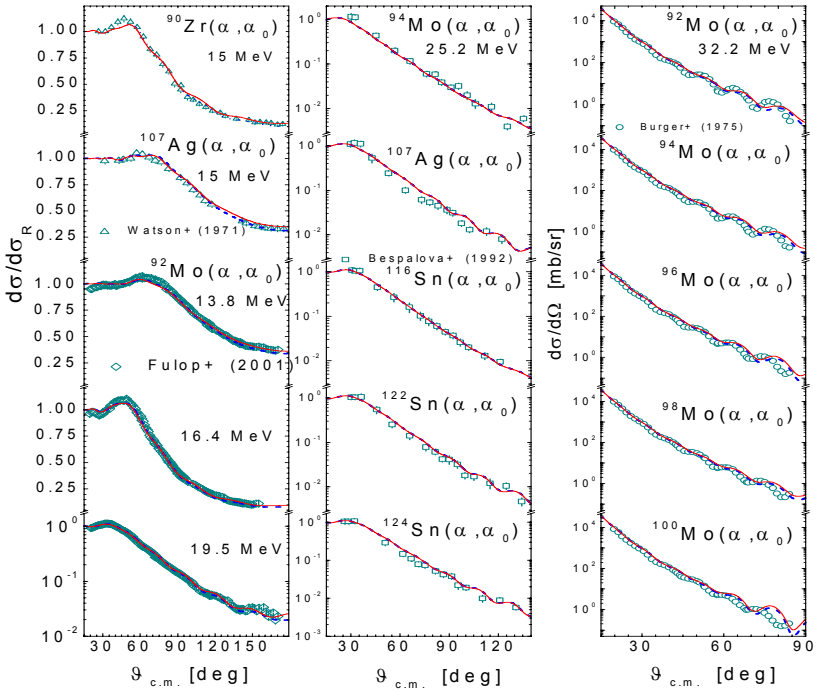

Density and energy-dependent effective NN-interaction[1]

$$v_{eff}^{D(EX)}(\rho,E,r) = F(\rho)g(E)v^{D(EX)}(r)$$

- $F(\rho)=C[1+\alpha e^{-\beta\rho}]$ (**DDM3Y**)
  $C[1-\alpha\rho]$ (**BDM3Y**)
- $g(E)$= 1-0.002E/A (**Reid NN** interaction)
  1-0.003E/A (**Paris NN** interaction)

[1] **G. Bertsch et al., Nucl.Phys. A284, 399 (1977);**
G.R. Satchler and W.G. Love, Phys. Rep. 55, 183 (1979);
N. Anantaraman et al., Nucl. Phys. A398, 269 (1983);
M.E. Brandan and G.R. Satchler, Phys. Rep. 285, 143, 1997;
Dao T. Khoa and G.R. Satchler, Nucl. Phys. A668, 3 (2000).

Density dependent NN-Reid effective interaction

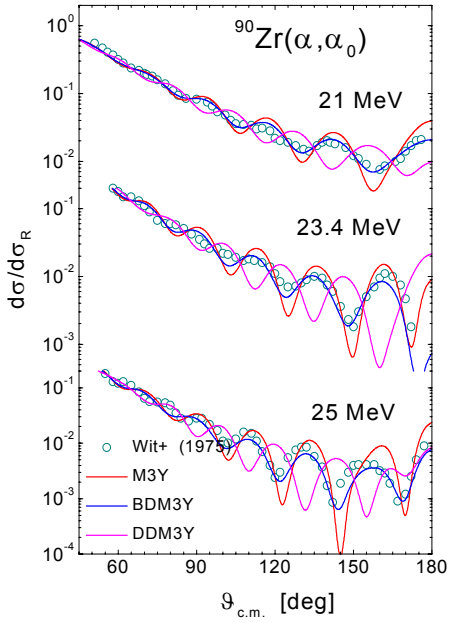

M. Avrigeanu, Research Co-ordination Meeting RIPL-3, Vienna, June 2004 15

Phenomenological optical potential

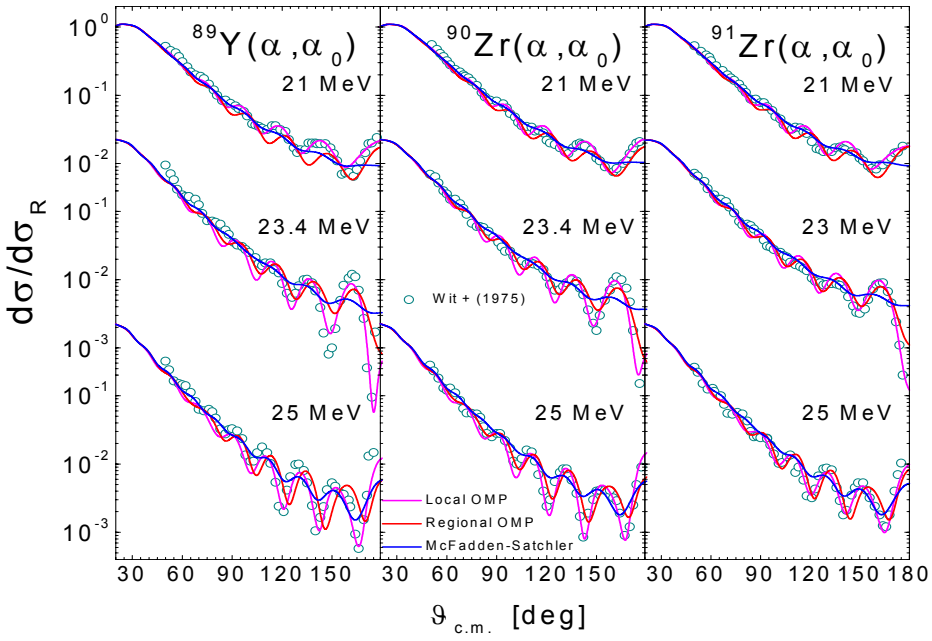

M. Avrigeanu, Research Co-ordination Meeting RIPL-3, Vienna, June 2004 16

Phenomenological optical potential

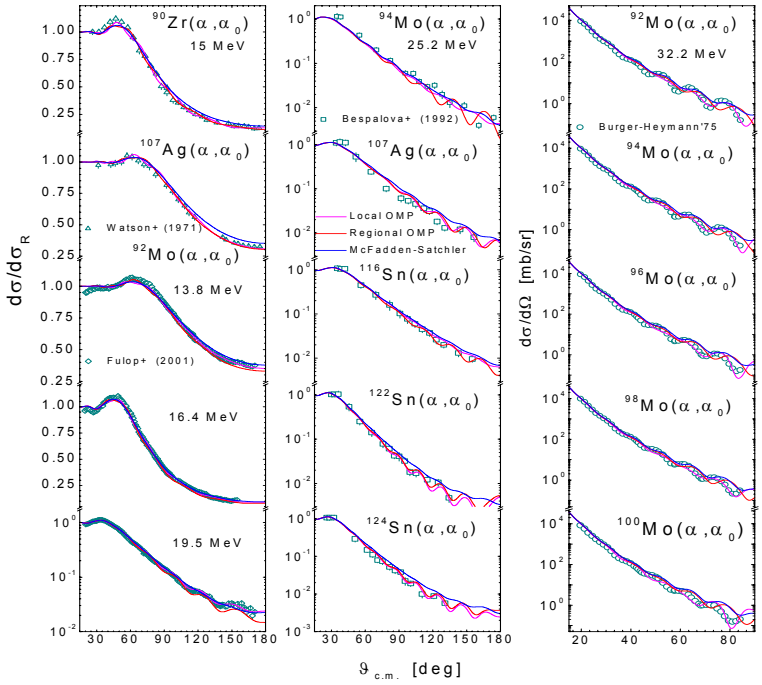

Microscopic & phenomenological real optical potential

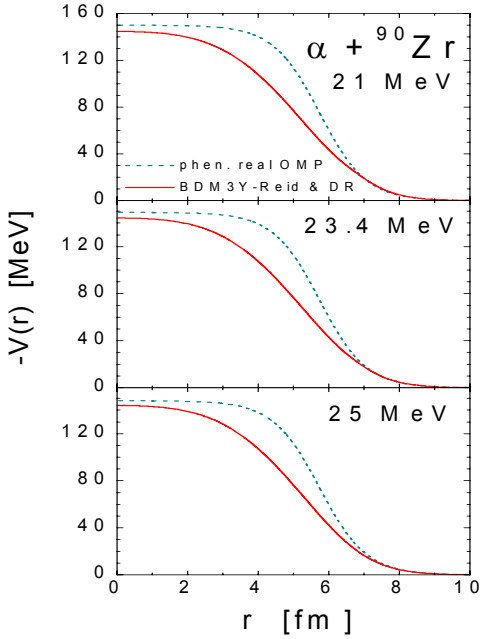

DF-equivalent Woods-Saxon real potential

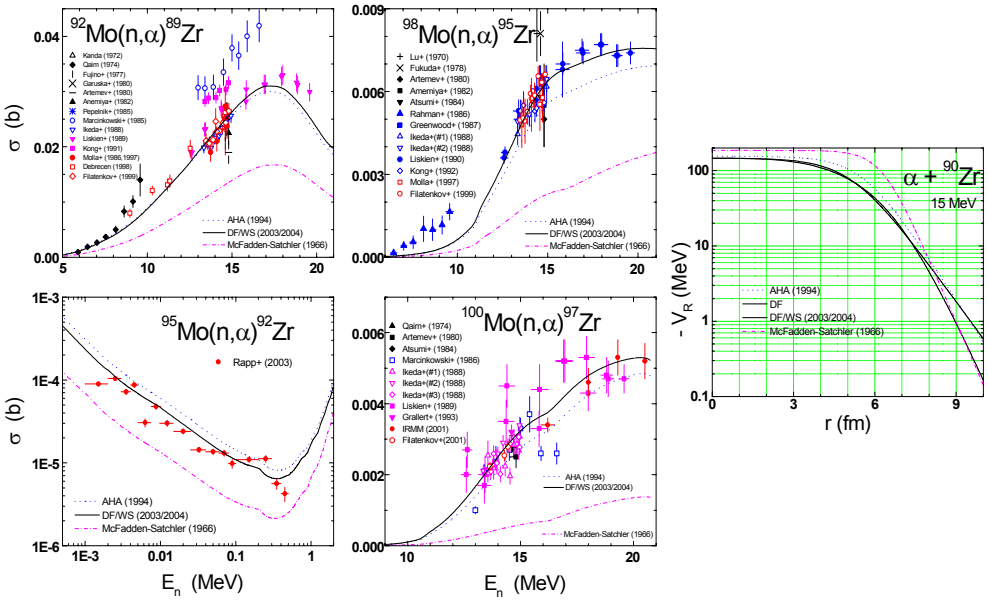

DF-equivalent Woods-Saxon real potential vs. phenomenological OMP based on (α,α_0) analysis

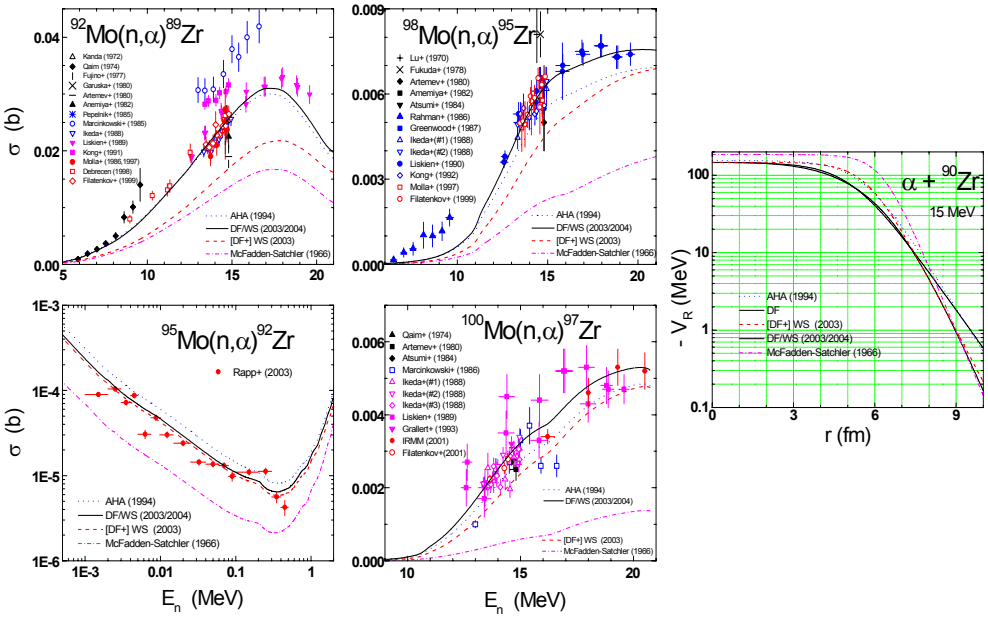

Conclusions

- α-α elastic-scattering at incident energies below 35 MeV (reaction threshold):
  - no coupling of phenomenological imaginary optical potential necessar
  - unambiguous informations about the ingredients of the folding procedure
    - effective NN-interaction : **M3Y-Reid**
    - density distribution of the alpha-particle : **Baye**-density
- α-particle elastic scattering on A<100 nuclei at energies below 32 MeV
  - DF approach using Reid effective interaction and Baye density distribution
  - DF-approach: the **number of free parameters decreased** by adjusting only the imaginary OMP part parameters
    - **energy-dependent** phenomenological OMP imaginary part
    - density dependence of the effective NN-interaction : **BDM3Y**-Reid
    - **dispersive correction** to the DF real potential
  - Full global parameter set: by adjusting only the real phenomenological potential parameters while the imaginary components remained unchanged:
    ~DF within the nuclear-surface tail region
  - DF-equivalent Woods-Saxon potential: ~DF within the nuclear surface region
- **(n,α) reaction cross sections for ^{92,95,98,100}Mo:** ***described by DF-equivalent WS potential***
  - ***frame:*** unitary analysis of all open reaction channels and stable isotope chain
    [http://tandem.nipne.ro/~vavrig/Publications/2003/]
- **Further work :** the whole mass range as well as the energies between 40 and 80 MeV.

M. Avrigeanu, Research Co-ordination Meeting RIPL-3, Vienna, June 2004 21

Appendix 3.3.

Vibrational enhancement of nuclear level density within response function method

V.A. Plujko and O.M. Gorbachenko

Vibrational enhancement of nuclear level density within response function method

V.A. PLUJKO, O.M. GORBACHENKO

Nuclear Physics Department, Taras Shevchenko National University,
Pr. Acad. Glushkova, 2, bdg.11, 03022 Kiev, Ukraine

E-mail: plujko@univ.kiev.ua

The main results are summarized on development of response function (RF) method for description of the vibrational state effects on nuclear level density. The enhancement factors calculated within different approaches are compared. The results of the RF approach are in the better agreement with that ones within method of attenuated phonon occupation numbers. They also agree reasonably with results of a finite temperature extension of the interacting boson model.

Level density ρ is one of the main quantities to define characteristics of nuclear decay. The collective states can strongly effect on level density, specifically, at low excitation energies ([1]-[6]). Calculation of the enhancement (variation) factor K of level densities is the simplest method to estimate effect of the vibrational states on level densities. The factor K is the ratio of level densities with and without allowing for vibrational states. The level densities can be calculated within framework of statistical approach by the use of standard saddle-point method [1] or its modification [7]. It was found [8] that factor K is practically independent of type of statistical approach. Therefore we use standard saddle-point method as a simplest way for calculation of the enhancement factor of level density.

In this contribution the effect of the vibrational state on nuclear level density is studied on the base of response function approach. The method allows to take into account the damping of vibrational states in a rather accurate way.

As it is mentioned before, enhancement factor of level density is given by the following expression

$$K = \rho / \rho_0 , \tag{1}$$

where ρ and ρ_0 are level densities with and without allowing for vibrational states. The level density is presented in the following form (within framework of statistical approach in standard saddle-point method[1]):

$$\rho(U, A) = \left(4\pi^2 D\right)^{-1/2} \exp S(\alpha_0, \beta_0), \tag{2}$$

where $S(\alpha_0,\beta_0)$ is entropy of nucleus with mass number A at excitation energy $U = E - E_{g.s.}$ with $E_{g.s.}$ for ground state energy,

$$S(\alpha_0,\beta_0) = -\alpha_0 A + \beta_0 E + \ln Z(\alpha_0,\beta_0) = \\ = -\alpha_0 A + \beta_0 E - \beta_0 \Omega(\alpha_0,\beta_0) \quad (3)$$

Here, $Z(\alpha,\beta)$ - partition function,

$$Z(\alpha,\beta) = \mathrm{Tr}\left[\exp\left(-\beta\hat{H} + \alpha\hat{A}\right)\right] \equiv \mathrm{Tr}\left[\exp\left(-\beta\tilde{H}\right)\right],\ \tilde{H} \equiv \hat{H} - \mu\hat{A},\ \ \mu = \alpha/\beta \quad (4)$$

and

$$\Omega(\alpha,\beta) = -\frac{1}{\beta}\ln Z(\alpha,\beta) \quad (5)$$

is the thermodynamic potential. The symbol "Tr" in (4) is the trace over all variables of all particles; $\hat{H}$ is the hamiltonian; $\hat{A}$ - operator of particle number. The function D in (1) is determinant of second partial derivatives of partition function logarithms with respect to parameters α and β. The saddle-point parameters α_0, β_0 define temperature ($T = 1/\beta_0$) and chemical potential ($\mu = \alpha_0/\beta_0$). They are solutions of the system of thermodynamic state equations

$$A = \frac{\partial}{\partial\alpha}\ln Z = -\frac{\partial}{\partial\alpha}\left[\beta\Omega\right], \quad E = -\frac{\partial}{\partial\beta}\ln Z = \frac{\partial}{\partial\beta}\left[\beta\Omega\right]. \quad 6)$$

We fellow random phase approximation (RPA) and consider vibrational states of the multipolarity L as collective states formed by two-body coherent interaction $V^k_{res}(i,j)$ of separable form:

$$V^k_{res}(i,j) = k\sum_{\mu=-L}^{+L} q^*_{L\mu}(\vec{r}_i)q_{L\mu}(\vec{r}_j),\ q_{L\mu}(\vec{r}) = r^L Y_{L\mu}(\hat{r})\ , \quad (7)$$

where $k \equiv k(L)$ is a coupling constant for nucleon-nucleon (coherent) interaction (1) with one-body operator $q_{L\mu}(\vec{r})$ of multipolarity L for form-factor. The total nuclear hamiltonian is equal to

$$\hat{H} = \hat{H}_0 + \hat{V}_{res} \equiv \hat{H}_k\ ,$$

$$\hat{V}_{res} \equiv \hat{V}^k_{res} = \frac{1}{2}\sum_{i,j} V^k_{res}(i,j) = \frac{k}{2}\sum_{\mu,i,j} q^*_{L\mu}(\vec{r}_i)q_{L\mu}(\vec{r}_j) \equiv \frac{k}{2}\sum_{\mu}\hat{Q}^+_{L\mu}\hat{Q}_{L\mu}\ , \quad (8)$$

where $\hat{H}_0$ is the hamiltonian of the independent particle model; $\hat{Q}_{L\mu} \equiv \sum_j q_{L\mu}(\vec{r}_j)$.

The thermodynamic potential (5) can be presented in the following form

$$\Omega = \Omega_0 + \Delta\Omega, \quad (9)$$

where $\Omega_0 = -(1/\beta)\ln Z_0$ is the thermodynamic potential of the independent particle model and $\Delta\Omega = -(1/\beta)\ln\Delta Z$ is an addition to the thermodynamic potential Ω_0 due to

presence of the residual interaction $\hat{V}_{res}$. In order to obtain (9), we use the Bloch transformation and define the function

$$\Omega_\lambda = -\beta^{-1}\ln Z \equiv -\beta^{-1}\ln \mathrm{Tr}\Big[\exp(-(\tilde{H}_0 + \lambda\hat{V}_{res})\beta)\Big],\quad \tilde{H}_0 = \hat{H}_0 - \mu\hat{A}\ , \qquad (10)$$

with additional factor λ at interaction. This function coincedes with Ω_0 and Ω at $\lambda = 0$ and $\lambda = 1$ respectively:

$$\Omega_0 \equiv \Omega_{\lambda=0}\ ,\quad \Omega \equiv \Omega_{\lambda=1}\ . \qquad (11)$$

Differentiation (11) with respect to λ leads to the expression

$$\frac{\partial\Omega}{\partial\lambda} = \mathrm{Tr}\hat{V}_{res}\exp(-(\tilde{H}_0 + \lambda\hat{V}_{res})\beta)/\mathrm{Tr}\exp(-(\tilde{H}_0 + \lambda\hat{V}_{res})\beta) =$$

$$\equiv \mathrm{Tr}\hat{V}_{res}\exp(-(\tilde{H}_0 + \hat{V}_{res}^{k'})\beta)/\mathrm{Tr}\exp(-(\tilde{H}_0 + V_{res}^{k'})\beta) \equiv <V_{res}>_{k'},\ \ k' = \lambda k\ , \qquad (12)$$

and after integration (12) in the range $\lambda = 0 \div 1$ we obtain

$$\Delta\Omega = \Omega_{\lambda=1} - \Omega_{\lambda=0} = \int_0^1 \frac{\partial\Omega}{\partial\lambda}\mathrm{d}\lambda = \int_0^1 <\hat{V}_{res}^{k}>_{k'=\lambda k}\ \mathrm{d}\lambda \equiv$$
$$\equiv \int_0^k \frac{<\hat{V}_{res}^{k'}>_{k'}}{k'}\mathrm{d}k'. \qquad (13)$$

With use of the Eq.(8), we find the following expression for thermodynamic potential addition $\Delta\Omega_L$ due to presence of the vibrational states with multipolarity L

$$\Delta\Omega = -(1/\beta)\ln\Delta Z \equiv \Delta\Omega_L = \sum_\mu \int_0^k dk' \left\langle \hat{Q}_{L\mu}^{*}\hat{Q}_{L\mu}\right\rangle_{k'}/2\ . \qquad (14)$$

Here, the bracket $\langle ... \rangle_{k'}$ denotes averaging on canonical ensemble with the density matrix $\hat{\rho} = \exp(-\beta\tilde{H}_{k'})/\mathrm{Tr}(\exp(-\beta\tilde{H}_{k'}))$, where $\tilde{H}_{k'} = \hat{H}_{k'} - \mu\hat{A}$; $\hat{H}_{k'}$ is total hamiltonian (1) with separable interaction constant k'.

The average quantity $\left\langle \hat{Q}_{L\mu}^{*}\hat{Q}_{L\mu}\right\rangle_{k'}$ in (14) can be identified with correlation function $\left\langle \hat{Q}_{L\mu}^{+}(t)\hat{Q}_{L\mu}(t')\right\rangle_{k'}$ at $t = t' + 0$,

$$\sum_\mu \left\langle \hat{Q}_{L\mu}^{*}\hat{Q}_{L\mu}\right\rangle_{k'} =$$
$$= \mathrm{Re}\sum_\mu \lim_{\tau\to+0}\left\langle \hat{Q}_{L\mu}^{+}(t+\tau)\hat{Q}_{L\mu}(t)\right\rangle_{k'} = \mathrm{Re}\sum_\mu \lim_{\tau\to+0}\left\langle \hat{Q}_{L\mu}^{+}(\tau)\hat{Q}_{L\mu}(0)\right\rangle_{k'}, \qquad (15)$$

where $\hat{Q}_{L\mu}(t) = \exp(iH_{k'}t/\hbar)\hat{Q}_{L\mu}\exp(-iH_{k'}t/\hbar)$ is the multipole operator in the Heisenberg representation the index (+) denotes Hermitian conjugation. The definition (15) corresponds to standard rules of the transition from average quantities to correlation functions within Green's function method ([9] –[11]): operators $Q_{L\mu}^{+}(t')$, $\hat{Q}_{L\mu}(t)$ are considered as

operators of a creation and annihilation of the phonons and annihilation operator acts before the creation operator; the cyclic properties of the trace are used to change from the Schroedinger to Heisenberg picture; the symbol of the real part is explicitly indicated because the quantity from left hand side of the Eq.(15) should be real.

Next we express this correlation function $\left\langle \hat{Q}^{+}_{L\mu}(t)\hat{Q}_{L\mu}(t')\right\rangle_{k'}$ through the linear response function $\chi_L(\omega)$ of the system with the hamiltonian (8) on external multipole field $\hat{Q}_{L\mu}$. In order to perform this transformation we use of the Green's function method ([9],[10]) and rewrite correlation function (15) by means of spectral function $I_{\hat{Q}^{+}_{L\mu}\hat{Q}_{L\mu}}$,

$$I_{\hat{Q}^{+}_{L\mu}\hat{Q}_{L\mu}}(\omega)=\sum_{\nu_1,\nu_2}\left\langle \nu_1\left|\hat{Q}^{+}_{L\mu}(0)\right|\nu_2\right\rangle\left\langle \nu_2\left|\hat{Q}_{L\mu}(0)\right|\nu_1\right\rangle\rho_{\nu_1,\nu_1}\delta\left(\varepsilon_{\nu_1}/\hbar-\varepsilon_{\nu_2}/\hbar-\omega\right), \quad (16)$$

in the following form

$$\sum_{\mu}\left\langle \hat{Q}^{*}_{L\mu}\hat{Q}_{L\mu}\right\rangle_{k'}=\mathrm{Re}\sum_{\mu}\lim_{\tau\to+0}\int_{-\infty}^{+\infty}I_{\hat{Q}^{+}_{L\mu}\hat{Q}_{L\mu}}(\omega)\cdot \mathrm{e}^{-i\omega\tau}\cdot\exp[\beta\hbar\omega]d\omega. \quad (17)$$

The quantities $|\nu\rangle$ and ε_ν in (16) are the wave function and energy of the total hamiltonian $H_{k'}$, (8); note that below we will often simplify denotation and omit the index k'. With the use of this expression we find that the thermodynamic potential addition $\Delta\Omega_L$,(14), is determined by spectral functions $I_{\hat{Q}^{+}_{L\mu}\hat{Q}_{L\mu}}$:

$$\Delta\Omega_L=\mathrm{Re}\sum_{\mu}\lim_{\tau\to+0}\int_{-\infty}^{+\infty}I_{\hat{Q}^{+}_{L\mu}\hat{Q}_{L\mu}}(\omega)\cdot \mathrm{e}^{-i\omega\tau}\cdot\exp[\beta\hbar\omega]d\omega/2. \quad (18)$$

In spherical nuclei spectral functions should be independent on magnetic quantum number μ and we have

$$\Delta\Omega_L=\frac{2L+1}{2}\mathrm{Re}\lim_{\tau\to+0}\int_{0}^{k}dk'\int_{-\infty}^{+\infty}I_{\hat{Q}^{+}_{L0}\hat{Q}_{L0}}(\omega)\cdot \mathrm{e}^{-i\omega\tau}\cdot \mathrm{e}\exp[\beta\hbar\omega]d\omega. \quad (19)$$

The spectral function $I_{\hat{A}\hat{B}}(\omega)$ is connected with the Fourier transforms $<<\hat{A},\hat{B}>>^{ret,adv}_{\omega}$ of the double-time retarded and advanced Green's functions $<<\hat{A}(t),\hat{B}(t')>>^{ret,adv}$ by the expression:

$$I_{\hat{A}\hat{B}}(\omega)=\frac{i\hbar}{e^{\beta\omega}-1}\left(<<\hat{A},\hat{B}>>^{ret}_{\omega}-<<\hat{A},\hat{B}>>^{adv}_{\omega}\right). \quad (20)$$

The Fourier transforms $<<\hat{A},\hat{B}>>^{ret,adv}_{\omega}$ are defined as

$$<<\hat{A},\hat{B}>>^{ret,adv}_{\omega}=(2\pi)^{-1}\int_{-\infty}^{+\infty}<<\hat{A}(t),\hat{B}(t')>>^{ret,adv}\exp(i\omega(t-t'))d(t-t') \quad (21)$$

with double-time Green's functions

$$<<\hat{A}(t),\hat{B}(t')>>^{ret,adv}=<[\hat{A}(t),\hat{B}(t')]>\times\begin{cases}-(i/\hbar)\theta(t-t'), & retarded,\\ +(i/\hbar)\theta(t'-t), & advanced,\end{cases} \quad (22)$$

where $\hat{A}(t), \hat{B}(t)$ are the Heisenberg operators; $[\hat{A}(t), \hat{B}(t')]$ is the commutator of the operators $\hat{A}$, $\hat{B}$; $\theta(t)$ is the Heaviside step function. The equation (20) is resulted from the relationships

$$<< \hat{A}, \hat{B} >>_{\omega}^{adv,red} = \pm i\left(e^{\beta\hbar\omega} - 1\right) I_{\hat{A}\hat{B}}(\omega)/(2\hbar) + \\ +(2\pi)^{-1} P \int_{-\infty}^{+\infty} \left(e^{\beta\hbar\omega'} - 1\right) I_{\hat{A}\hat{B}}(\omega') d\omega'/(\omega - \omega'). \tag{23}$$

With definition (16), the spectral function $I_{\hat{Q}_{L0}^{+}\hat{Q}_{L0}}$ is real non-negative quantity. Therefore the Eq.(23) shows that the function $I_{\hat{Q}_{L0}^{+}\hat{Q}_{L0}}$ is directly related with the imaginary part of the retarded or advanced Green's functions by the formula

$$I_{\hat{Q}_{L0}^{+}\hat{Q}_{L0}}(\omega) = -\frac{2\hbar}{e^{\beta\hbar\omega} - 1} Im << \hat{Q}_{L0}^{+}, \hat{Q}_{L0} >>_{\omega}^{ret}. \tag{24}$$

According to linear response theory ([9],[10]), the retarded Green's function $<< \hat{Q}_{L0}^{+}, \hat{Q}_{L0} >>_{\omega}^{ret}$ is proportional to linear response function $\chi_L^{k'}(\omega)$ (RF),

$$<< \hat{Q}_{L0}^{+}, \hat{Q}_{L0} >>_{\omega}^{ret} = \chi_L^{k'}(\omega)/2\pi, \tag{25}$$

of a system with the hamiltonian $H_{k'} = H_0 + V_{res}^{k'}$ on the external field

$$\hat{V}_L^{ext}(t) = b_{\omega}(t)\hat{Q}_{L0}, \quad b_{\omega}(t) = b_0 \exp\left[-i\left(\omega + i\delta\right)t\right], \quad b_0 \ll 1, \ \delta \to +0 \ . \tag{26}$$

The linear response function $\chi_L^{k'}(\omega)$ determines a linear variation of the average value $< \hat{Q}_{L0}^{+} >_{k'}$ of the multipole momentum $\hat{Q}_{L0}^{+}$ under action of the external field $\hat{V}_L^{ext}(t)$:

$$\delta < \hat{Q}_{L0}^{+}(t) >_{k'} = e^{-i(\omega+i\delta)t} \cdot \chi_L^{k'}(\omega) \equiv 2\pi \, e^{-i(\omega+i\delta)t} << \hat{Q}_{L0}^{+}, \hat{Q}_{L0} >>_{\omega}^{ret}. \tag{27}$$

It has the following explicit form

$$\chi_L^{k'}(\omega) = \mathrm{Tr}\left(\hat{Q}_L\{\vec{r}_j\} \cdot \delta\rho_{\{A\}}(\{\vec{r}_j\};\omega)\right) = \mathrm{Tr}_{\{1\}}\left(q_{L0}(\vec{r}) \cdot \delta\rho(\vec{r};\omega)\right), \tag{28}$$

where $\delta\rho_{\{A\}}(\{\vec{r}_j\};\omega)$, $\delta\rho(\vec{r};\omega)$ are many-body and one-body transition densities. They are related with the Fourier transforms $\delta\overline{\rho}_{\{A\}}(\{\vec{r}_j\};\omega)$, $\delta\overline{\rho}(\vec{r};\omega)$ of the variations of the many-body and one-body densities under acting of the external field (26):

$$\delta\rho_{\{A\}}(\{\vec{r}_j\};\omega) \equiv \delta\overline{\rho}_{\{A\}}(\{\vec{r}_j\};\omega)/b_0 \ , \ \ \delta\rho(\vec{r};\omega) \equiv \mathrm{Tr}_{\{\text{A-1}\}}\left[\delta\rho_{\{A\}}(\vec{r}, \{\vec{r}_{l=1\div A-1}\};\omega)\right] = \\ = \delta\overline{\rho}(\vec{r};\omega)/b_0, \ \delta\overline{\rho}(\vec{r};\omega) \equiv \mathrm{Tr}_{\{\text{A-1}\}}\left[\delta\overline{\rho}_{\{A\}}(\vec{r}, \{\vec{r}_{l=1\div A-1}\};\omega)\right] . \tag{29}$$

The symbols $\mathrm{Tr}_{\{1\}}$, $\mathrm{Tr}_{\{\text{A-1}\}}$ in (28) and (29) are the partial traces over one-indicated variable and $A-1$ variables respectively.

With the use of the Eq.(25) we have the following expression for the addition $\Delta\Omega_L$, (19), to the thermodynamic potential

$$\Delta\Omega_L = \frac{2L+1}{2\pi}\mathrm{Re}\lim_{\tau\to+0}\int_0^k dk'\int_{-\infty}^{+\infty}\frac{\hbar}{1-e^{-\beta\hbar\omega}}\cdot \mathrm{e}^{-i\omega\tau}\cdot \mathrm{Im}\chi_L^{k'}(\omega)d\omega\,. \qquad (30)$$

The addition $\Delta\Omega_L$ can be evaluated in the two ways: 1) to perform direct integration (30) over real frequency ω; 2) to use the contour integration in the complex frequency plane; the convergence factor $\exp(-i\omega\tau)$ with $\tau > 0$ defines the appropriate contour and the integration counter should be closed in the lower half-plane of the complex ω-plane due to presence this factor. Similar to the retarded (advanced) Green's function, the linear response function $\chi_L^{k'}(\omega)$ (complex conjugate response function $\chi_L^{k'^*}(\omega)$) is analytical in the upper (lower) ω-half-plane but has the poles in the lower (upper) ω-half-plane. The asymptotic behavior of the response functions is the same one as that of the Green's functions and in general case ([11],[12])

$$\chi_L^{k'}(\omega) \propto <<\hat{Q}_{L0}^{+},\hat{Q}_{L0}>>_{\omega}^{ret} \sim 1/\omega, \quad |\omega|\to\infty,$$
$$\chi_L^{k'^*}(\omega) \propto <<\hat{Q}_{L0}^{+},\hat{Q}_{L0}>>_{\omega}^{adv} \sim 1/\omega, \quad |\omega|\to\infty. \qquad (31)$$

Note that the nuclear response functions in physical meaningful cases are satisfied the energy weighted sum rules of the form (in cold nuclei [13])

$$\int_0^{+\infty}\omega\cdot \mathrm{Im}\chi_L^{k'}(\omega)d\omega = const\,. \qquad (32)$$

It means that in the realistic situations the imaginary part of RF should tend to zero faster than $1/\omega$ at large frequencies,

$$\mathrm{Im}\,\chi_L^{k'}(\omega) \sim 1/\omega^{1+\varepsilon},\ \varepsilon > 0, \quad |\omega|\to\infty. \qquad (33)$$

In these cases the symbols of the limit and real part in the Eq. (30) can be omitted and the expression (30) for the addition to the thermodynamic potential takes the form

$$\Delta\Omega_L = \frac{2L+1}{2\pi}\int_0^k dk'\int_{-\infty}^{+\infty}\frac{\hbar}{1-e^{-\beta\hbar\omega}}\cdot \mathrm{Im}\chi_L^{k'}(\omega)d\omega\,. \qquad (34)$$

This expression can be evaluated by counter integration with the closing the integration counter in any suited half-plane of the complex ω -plane due to the vanishing contribution from counters with $|\omega|\to\infty$.

The relationship (35) can be rewritten in the following form convenient for performing numerical integration with respect to real frequency:

$$\Delta\Omega_L = \frac{2L+1}{2\pi}\int_0^k dk'\int_0^{+\infty}\mathrm{cth}\left(\frac{\beta\hbar\omega}{2}\right)\cdot \mathrm{Im}\chi_L^{k'}(\omega)d(\hbar\omega)\,, \qquad (35)$$

where the symmetry relation $\mathrm{Im}\chi_L^{k'}(-\omega) = -\mathrm{Im}\chi_L^{k'}(\omega)$, $\omega \equiv \mathrm{Re}$, was used for transformation Eq.(34) to (35).

The addition $\Delta\Omega_L$ to the thermodynamic potential should be equal to zero in the absence of the coherent interaction. In order to provide this condition we modify expressions

(30), (35) and subtract from their integrands of a contribution corresponding to response function $\chi_L^{k'=0}(\omega)$ of the independent particle model without forming collective states, so that instead of the Eq.(30), (34), (35) we use the following expressions:

$$\Delta\Omega_L = \frac{2L+1}{2\pi}\mathrm{Re}\lim_{\tau\to+0}\int_0^k dk'\int_{-\infty}^{+\infty}\frac{\hbar}{1-e^{-\beta\hbar\omega}}\cdot \mathrm{e}^{-i\omega\tau}\cdot \mathrm{Im}\left\{\chi_L^{k'}(\omega)-\chi_L^{k'=0}(\omega)\right\}d\omega\,, \quad (36)$$

$$\Delta\Omega_L = \frac{2L+1}{2\pi}\int_0^k dk'\int_{-\infty}^{+\infty}\frac{\hbar}{1-e^{-\beta\hbar\omega}}\cdot \mathrm{Im}\left\{\chi_L^{k'}(\omega)-\chi_L^{k'=0}(\omega)\right\}d\omega\,, \quad (37)$$

$$\Delta\Omega_L = \frac{2L+1}{2\pi}\int_0^k dk'\int_0^{+\infty}\mathrm{cth}\left(\frac{\beta\hbar\omega}{2}\right)\cdot \mathrm{Im}\left\{\chi_L^{k'}(\omega)-\chi_L^{k'=0}(\omega)\right\}d(\hbar\omega)\,. \quad (38)$$

The expressions (36)-(38) are contributions to the thermodynamic potential from vibrational states with fixed multipolarity L. The overall addition to the thermodynamic potential determining change of the total level density due to presence of the vibrational states is the sum of $\Delta\Omega_L$,

$$\Delta\Omega = \sum_L \Delta\Omega_L\,, \quad (39)$$

and total thermodynamic potential with allowance for the vibrational states is given by (9). Then the level density is calculated using the equations (2)-(6), i.e., a variation of the temperature due to presence of the collective states is also taken into account. The vibrational enhancement factor is found from the eq.(1) as a ratio of the level densities with (ρ) and without (ρ_0) allowing for vibrational states. The expressions of the Fermi-gas model are used for calculation of the mean-field components of the thermodynamic potential Ω_0, the temperature and level density ρ_0.

We adopt a semiclassical approach based on the Landau-Vlasov kinetic equation to calculate nuclear response function $\chi_L^{\kappa}(\omega)$ ([14], [15]). Vibrational states are considered as collective states formed by coherent interactions of the separable form (8). Non-coherent residual interaction is taken into account for description of the collective state damping. The non-coherent residual interaction is included within relaxation time method with retardation effects during two-body collisions ([16]-[18]). It allows to consider the damping of vibrational states in a rather simple and accurate way. The RF has a general form($N = Z$)

$$\chi_L^{\kappa}(\omega) = \frac{\Pi_L(\omega)}{1-\kappa\,\Pi_L(\omega)},\quad \Pi_L(\omega)\equiv\chi_L^{\kappa=0}(\omega)\,. \quad (40)$$

Note that this form has also the nuclear response function within the RPA approach, but unlike the RPA response function, the semiclassical RF $\Pi_L(\omega)\equiv\chi_L^{\kappa=0}$ includes collective states damping ([16]- [18]).

There are simple methods for calculations of the vibrational enhancement factor K with approximate allowing for damping vibrational states ([3, [4], [6], [19]). They are based on different phenomenological extensions of the analytical boson-shape expression for vibrational enhancement factor. At first the effect of the vibrational state damping on

enhancement factor was considered in [3]. The complex energies of vibrational states in boson partition function were used and an expression for K had the following form:

$$K = K_{CE} \equiv \prod_L \left| \frac{1-\exp\left[-(\hbar\omega_L + i\gamma_L)/T\right]}{1-\exp\left[-(\hbar\tilde{\omega}_L + i\tilde{\gamma}_L)/T\right]} \right|^{-(2L+1)}, \quad (41)$$

where $\hbar\omega_L \equiv \hbar\omega_L(T)$ is temperature-dependent energy of the vibrational state with multipolarity L,

$$[\hbar\omega_L]^2 = [\hbar\tilde{\omega}_L]^2 - \xi(T)\{[\hbar\tilde{\omega}_L]^2 - [\hbar\omega_{L,\exp}]^2\},\ \xi(T) = \exp(-C_1 T^2/[\hbar\omega_{L,\exp}])\ ; \quad (42)$$

with $C_1 = 0.08\ MeV^{-1}$; $\hbar\tilde{\omega}_L$ - the average energy of the one-particle one-hole states,

$$\hbar\tilde{\omega}_L = \begin{cases} \hbar\omega_{shell}/2 \simeq 20 \cdot A^{1/3}, & L^\pi = 2^+, \\ \hbar\omega_{shell}, & L^\pi = 3^+. \end{cases} \quad (43)$$

The quantity $\hbar\omega_{L,\exp} \equiv \hbar\omega_L(T=0)$ is experimental value of the collective energy in cold nucleus; $\gamma_L = \bar{\gamma}(\omega_L, T)$, $\tilde{\gamma}_L = \bar{\gamma}(\tilde{\omega}_L, T)$ are damping coefficient of the vibrational state; the spreading $\bar{\gamma}(\omega, T)$ of the collective excitation was taken like that one for zero-sound damping in a Fermi liquid:

$$\bar{\gamma}(\omega, T) = C \cdot \left[(\hbar\omega)^2 + 4\pi^2 T^2 \right] \quad (44)$$

with $C = 0.013\ MeV^{-1}$.

Damped occupation numbers of boson states in the variation of entropy and excitation energy were used in expression for K considered in [6]:

$$K = K_{DN} \equiv \exp\left(\delta\bar{S} - \delta\bar{U}/T\right). \quad (45)$$

Here,

$$\delta\bar{S} = \sum_L (2L+1)\left[(1+n_L)\ln(1+n_L) - n_L \ln n_L\right], \quad \delta\bar{U} = \sum_L (2L+1)\hbar\omega_L n_L \quad (46)$$

- entropy and excitation energy phonon states with attenuated phonon occupation numbers

$$n_L = \frac{\exp\left[-\Gamma_L/(2\hbar\omega_L)\right]}{\exp(\hbar\omega_L/T) - 1}. \quad (47)$$

where damping width Γ_L has the form (44) with $C = 0.0075 A^{1/3}$ MeV^{-1}; the energy of vibrational states are taken from experimental systematics, for example, $\hbar\omega_{2^+} = 30 A^{-2/3}\ MeV$.

Attenuation of vibrational enhancement with temperature in form of a Fermi function is adopted in modular system EMPIRE-II of codes for nuclear reactions calculations [19]. The corresponding enhancement factor has the following form

$$K = K_{EM} \equiv K_{LDM}(1 - Q_{damp}) + Q_{damp}, \tag{48}$$

where K_{LDM} is the enhancement factor of surface vibrational states within the liquid drop model,

$$K_{LDM} = \exp\left[C_{4/3}\left(\frac{\rho_0}{\hbar^2 \sigma} \right)^{2/3} R_0^2 T^{4/3} \right] = \exp\left[C_3 A^{2/3} \cdot T^{4/3} \right] \tag{49}$$

with $C_{4/3} = \int_0^\infty x^{4/3}/(\exp(x) - 1)dx = 1.694$ and ρ_0 for nuclear mass density, σ for the surface tension coefficient; $C_3 = 0.06064\ MeV^{-4/3}$.

The quantity Q_{damp} in (49) is empirical factor of the vibrational enhancement damping. It is adopted in the form

$$Q_{damp} = 1/(1 + \exp(-(T - T_{1/2})/DT)), \tag{50}$$

where $T_{1/2} = 1$ MeV, $DT = 0.1$ MeV.

The calculations of the vibrational enhancement factor due to presence of the quadrupole 2^+ states within the RF method and different phenomenological approaches (41), (41), (48) are compared on the figures 1,2. The factors K are calculated for ^{56}Fe and ^{146}Sm. The coupling constants κ of the the coherent interaction were found from fitting of the peak energy of the strengh function, i.e., imaginary part of the RF (50), to the experimental energies $\hbar\omega_{2^+}$ in cold nuclei.

It can be seen that calculations within the RF approach agree better with that ones within method of the attenuated phonon occupation numbers (45)-(47). They also reasonably close to the results of a finite temperature extension of the interacting boson model ([20], [21]).

The calculations according to the RF approach were performed with different expressions for relaxation times τ of the collective states ([16]- [18]). We present on figs.1,2 the results with collective relaxation time according to kinetic approach with $\hbar/\tau$ of the form (44). The calculations within the RF method demonstrated rather strong dependence of the level density on the relaxation time shape. This can give additional possibility for investigation of the collective state relaxation in heated nuclei.

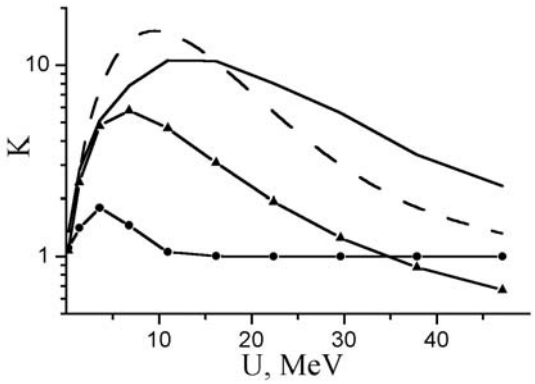

Fig.1 The dependence of the enhancement factor K on excitation energy for ^{56}Fe.

The curves: —— the RF method, – – – K_{DN}, —¡— K_{CE}, —¾— K_{EM}.

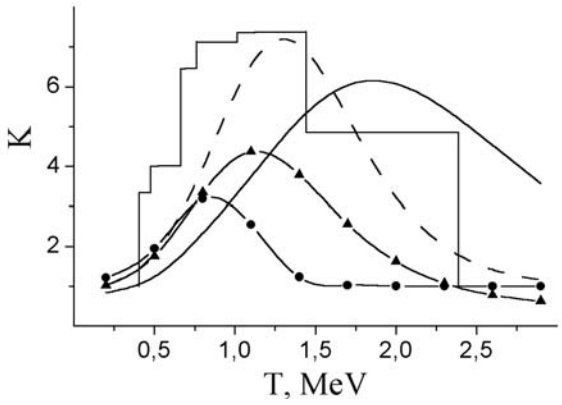

Fig.2 The dependence of the enhancement factor K on excitation energy for ^{146}Sm.

The curves: —— the RF method, – – – K_{DN}, —¡– K_{CE}, —¾– K_{EM};

histogram- calculations within temperature-dependent IBM model [21].

It seems that the method of the temperature dependent occupation numbers (45)-(47) are the best simple method of the enhancement factor calculations, but the more extensive studies are needed for more reliable conclusions.

This work is supported in part by the IAEA(Vienna) under Research Contract #12492/RO/RBF.

References

[1] Ignatyuk A.V., Statistical Properties of Excited Atomic Nuclei (in Russian). (Energoatomizdat, Moscow 1983); Transl. IAEA, Report INDC-233(L) (IAEA Vienna 1985).
[2] Vdovin A.I., Voronov V.V., Malov L.A., Solovyev B.G.,. Stoyanov Ch, Physics of Elementary Particles and Atomic Nuclei (Particles and Nucleus), 7(1976)952.
[3] Blokhin A.I., Ignatyuk A.V., Shubin Yu.N. Sov.J.Nucl.Phys., 48(1989)371.
[4] Ignatyuk A.V., V.P. Lunev V.P., Yu.N. Shubin Yu.N. Nuclear Theory for Fast Neutron Nuclear Data Evaluation, IAEA-TECDOC-483, Vienna. (1988)122.
[5] Ezhov S.N., Plujko V.A., Izv.Ros.Akad.Nauk. Ser.Fiz. 57(1993)78.
[6] Ignatyuk A.V., Weil J.L., Raman S., Kahane S., Phys. Rev. C47(1993)1504.
[7] Grossjean M.K., Feldmeier H., Nucl. Phys. A444(1985)113.
[8] Plujko V.A., Gorbachenko A.N., Izvestiya Rossiyskoy Academiyi Nauk. Seriya Fizicheskaya. 66(2002)1502; 67 (2003)1555; Ukrainian Journal of Physics. 48 (2003) 790.
[9] Bogolyubov N.N., Bogolyubov N.N., Jr., Introduction to Quantum Statistical Mechanics, World Scientific, (1983).
[10] Kubo R., Toda M., Hashitsume N. Statistical Physics II. Nonequilibrium statistical mechanics. Spinger-Verlag., NY, (1985).
[11] Fetter A.L., Walecka J.D. Quantum theory of many-particle systems. McGraw-Hill, Inc., NY, (1971).
[12] Zagoskin A.M. Quantum theory of many-body systems. Techniques and applications. Springer. (1998).
[13] Bohr A., Mottelson B.R. Nuclear structure. Benjamin, London, 2(1975).
[14] Brink D.B., Dellafiore A., Di Toro M., Nucl. Phys. A456(1986)205.
[15] Burgio G.F.,, Di Toro M., Nucl. Phys. A476(1988)189.
[16] Kolomietz V.M., Plujko V.A., Shlomo S., Phys. Rev. C54(1996)3014.
[17] Plujko V.A., Gorbachenko O.M., Kavatsyuk M.O., Acta Phys. Slov. 51(2001)231.
[18] Plujko V.A., et al., J.Phys.: CM, 14(2002)9473.
[19] Herman M., Capote-Noy R., Oblozinsky P., Trkov A., Zerkin V. Journal Nucl. Sci. Technol. V1. Suppl.2(2002)116; http://www-nds.iaea.org/empire/
[20] Mengoni A., Ventura A., Masetti S., Capote R., Kuznezov D. Journal Nucl. Sci. Thechnol. Suppl.2(August 2002)766.
[21] Capote R., Kusnezov D., Mengoni A., Ventura A. Proc. of 9-th Inter. Conf. on Nucl. React. Mech., Varenna, June 5-9, 2000. Ed. E. Gadioli. Universita degli Studi di Milano, 2000. Suppl. 115. P.125-134.

Appendix 3.4.

Some proposals for RIPL-3 development from Japan

T. Fukahori

Some Proposals for RIPL-3 Development from Japan

Tokio FUKAHORI
Nuclear Data Center, Japan Atomic Energy Research Institute
Tokai-mura, Naka-gun, Ibaraki-ken, 319-1195 Japan

1. Systematics for cross section calculations above 20 MeV

For various application related accelerator systems, JENDL High Energy File are preparing by Nuclear Data Center at Japan Atomic Energy Research Institute (JAERI/NDC) in cooperated with Japanese Nuclear Data Committee (JNDC). For this evaluation, the systematics calculating total, elastic and total reaction cross sections and angular distribution of elastic scattering for neutrons and protons is developed as TOTELA code. TOTELA can calculate above physical quantities for nuclides from C to U in the energy range from 20 MEV to 3 GeV. The example of result for Pb-208 is shown in **Fig.1** comparing with other systematics and experimental data. It can be seen that the TOTELA result can reproduce experimental data very well.

This program can be used to check optical model calculations by using RIPL parameters, especially in the case that there is no experimental data. TOTELA can be provided for RIPL-3.

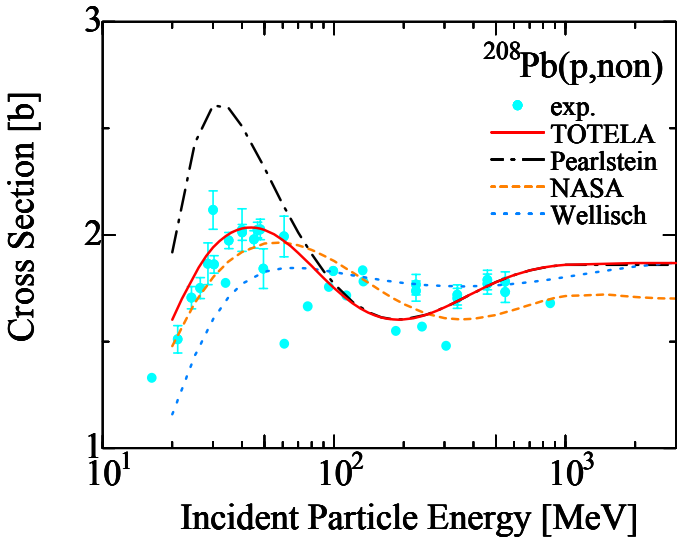

Fig.1 The example of result for Pb-208 calculated

2. Systematics for fission cross section calculations in intermediate energy region

For same requirement as TOTELA code, FISCAL code developed for the calculation of fission cross section in the intermediate energy region. As seen in **Fig.2**, if we can assume fission probabilities as a ratio of fission and total reaction cross sections in a function of excitation energy of fissioning nucleus, neutron-, proton- and poton-induced fission reactions have similar behavior. So, we can produce systematics as following equations from experimental data of fission cross section for ^{107}Ag-^{243}Am (63 data sets).

$$P_{fis}(Z,A,E) = p_1[1-exp\{-p_3(E-p_2)\}]$$

$$p_1 = [S + exp\{(q_{1,1} - x)/q_{1,2}\}]^{-1}$$

$$p_i = exp(q_{i,1} + q_{i,2}x) \qquad (i = 2,3, \qquad x = Z^2/A)$$

where P_{fis} is fission probability ($=\sigma_{fis}/\sigma_R$), σ_{fis} fission cross section, σ_R total reaction cross section, Z and A atomic and mass number of fissioning nuclei, E maximum excitation energy, S and $q_{i,j}$ fitting parameters.

FISCAL can be also usable to check the calculated results of fission cross sections by using RIPL-3 parameters. FISCAL can be also provided for RIPL-3.

3. Other proposals

In JAERI/NDC, nuclear data evaluation code like GNASH is under development. This code can be used for test calculations of RIPL-3 parameters.

In RIPL-2, there are some parameters not included, even for stable isotopes. To fill the lack of these, parameters can be added both to the database and systematics.

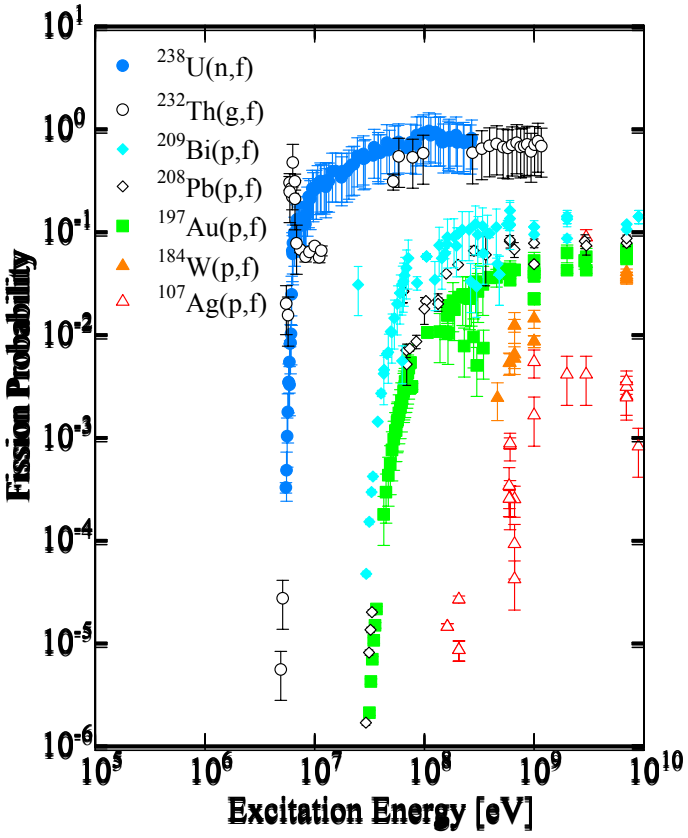

Fig.2 Trends of intermediate energy fission probability for neutron-, proton- and photon-induced reaction.

Improvement and addition of retrieval tools for www will be prepared for RIPL-3 database (as it was done for RIPL-2). A possibility to use unique file for each segment will be analyzed.

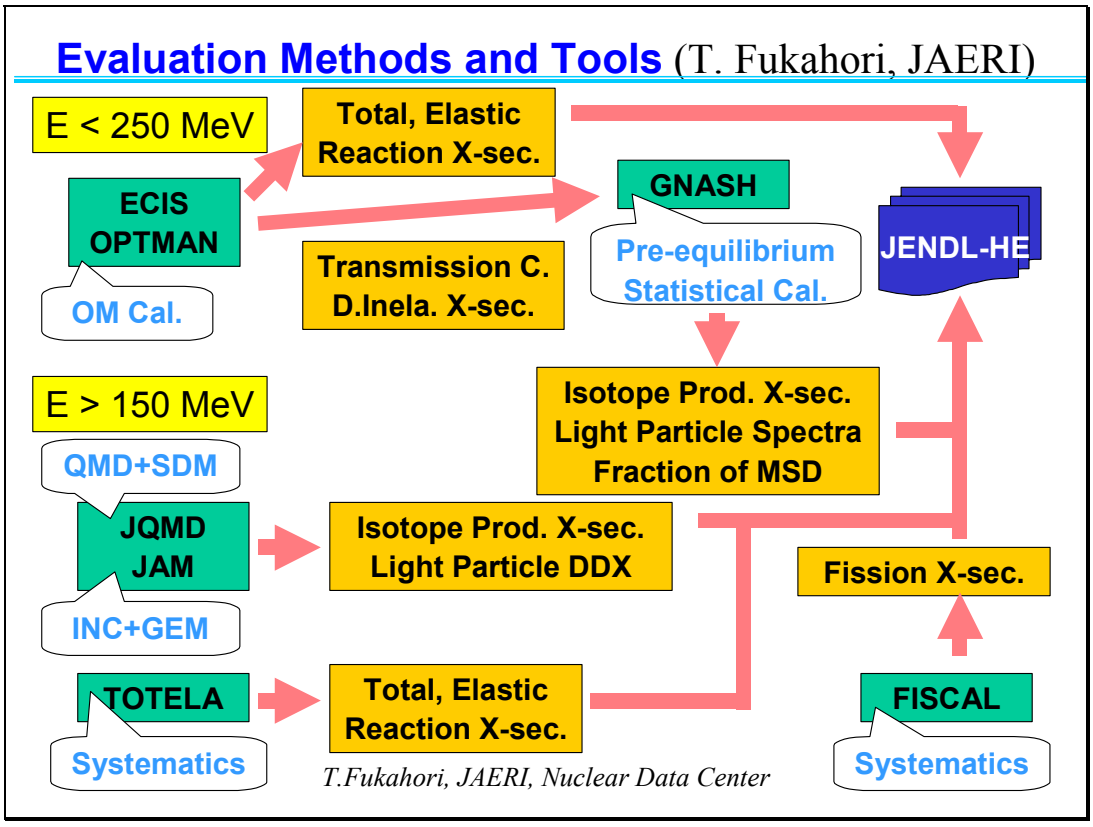
Evaluation Methods and Tools (T. Fukahori, JAERI)
E < 250 MeV
Total, Elastic Reaction X-sec.
ECIS OPTMAN
OM Cal.
GNASH
Pre-equilibrium Statistical Cal.
JENDL-HE
Transmission C. D.Inela. X-sec.
E > 150 MeV
QMD+SDM
Isotope Prod. X-sec. Light Particle Spectra Fraction of MSD
JQMD JAM
INC+GEM
Isotope Prod. X-sec. Light Particle DDX
Fission X-sec.
TOTELA
Systematics
Total, Elastic Reaction X-sec.
FISCAL
Systematics
T.Fukahori, JAERI, Nuclear Data Center

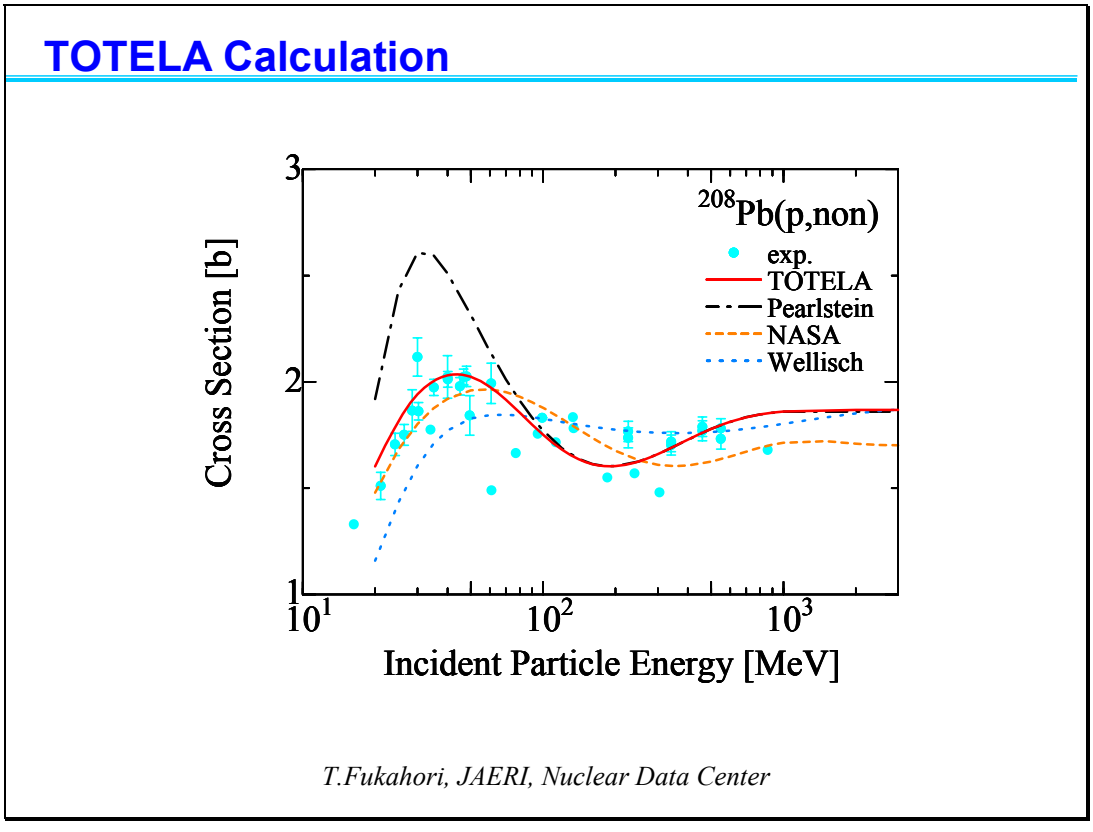
TOTELA Calculation
208Pb(p,non)
exp.
TOTELA
Pearlstein
NASA
Wellisch
Cross Section [b]
Incident Particle Energy [MeV]
T.Fukahori, JAERI, Nuclear Data Center

FISCAL Calculation (Introduction)

Assumption:
Fission Probability
Excitation Energy of
Fissioning Nucleus

→Proton-,
Neutron-, and
Photon-induced
Fission Reactions
have similar
behavior.

→Systematics

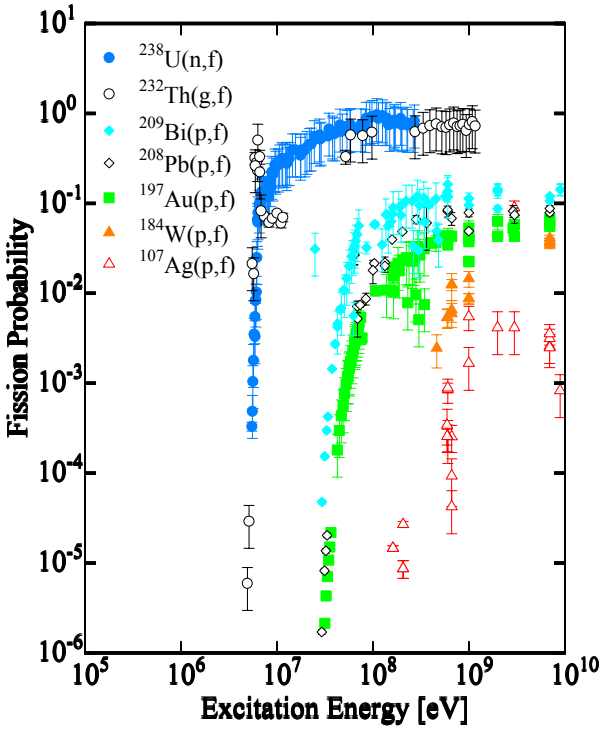

FISCAL Calculation (Systematics - Equation)

$$P_{fis}(Z,A,E) = p_1[1-exp\{-p_3(E-p_2)\}]$$

$$p_1 = [S + exp\{(q_{1,1} - x)/q_{1,2}\}]^{-1}$$

$$p_i = exp(q_{i,1} + q_{i,2}x) \qquad (i = 2,3, \qquad x = Z^2/A)$$

P_{fis} : Fission Probability(=σ_{fis}/σ_R)

σ_{fis} : Fission Cross Section 、 σ_R : Non-elastic Cross Section

Z、A : Atomic and Mass Number of Fissioning Nuclei

E : Maximum Excitation Energy、S, $q_{i,j}$: Fitting Parameter

Experimental data of proton, neutron and photon
induced fission cross section for ^{107}Ag～^{243}Am (63 data sets)

T.Fukahori, JAERI, Nuclear Data Center

FISCAL Calculation (Systematics – Results(1))

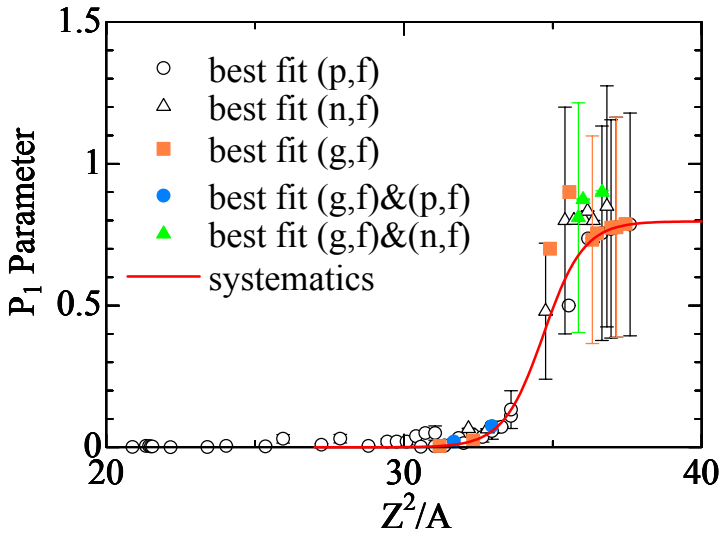

T.Fukahori, JAERI, Nuclear Data Center

FISCAL Calculation (Systematics – Results(2))

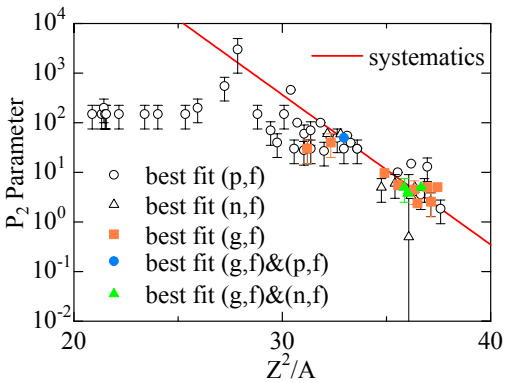

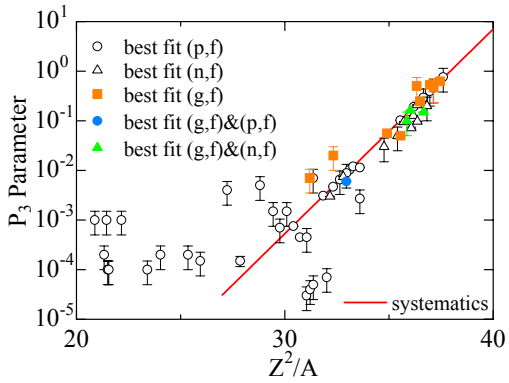

	S	$q_{i,1}$	$q_{i,2}$
p_1	0.797	34.7	0.676
p_2	-	26.8	-0.696
p_3	-	-36.0	0.949

T.Fukahori, JAERI, Nuclear Data Center

FISCAL Calculation (n-induced Cross Sections)

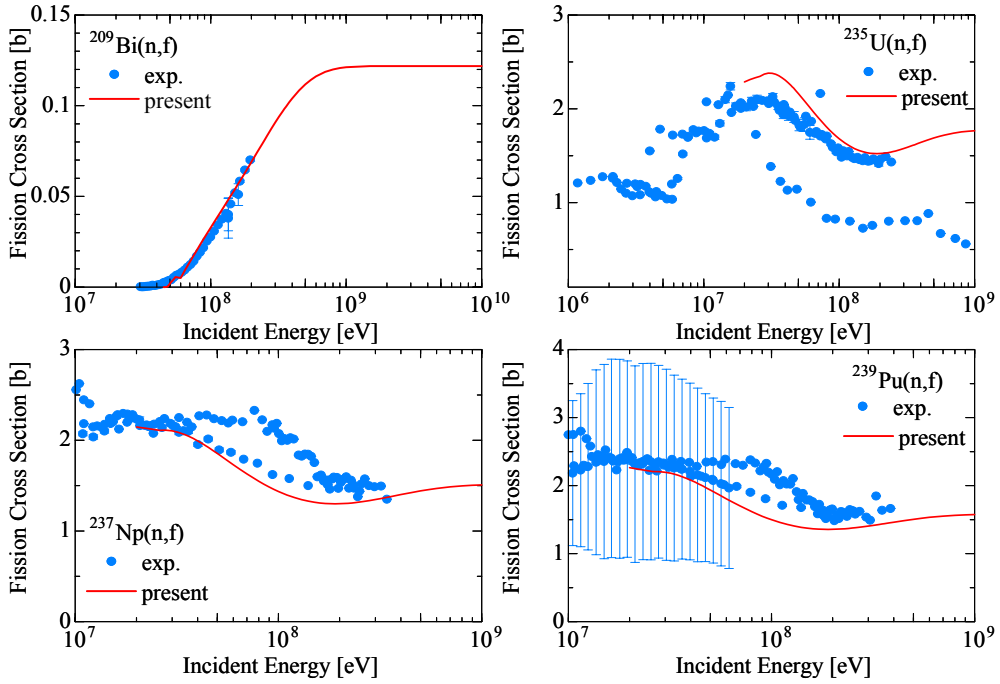

T.Fukahori, JAERI, Nuclear Data Center

Additional Proposals

- POD code development

test and usage of RIPL-3 parameters

- Adding parameters which are not included in RIPL-2

especially for stable isotopes

- Improvement and addition of retrieval tools and www

format consideration

unifying file of each segment ???

T.Fukahori, JAERI, Nuclear Data Center

Appendix 3.5

Level Densities: High energy behaviour and collective enhancement

R. Capote Noy

Level densities: High energy behaviour and collective enhancement

R. Capote
IAEA Nuclear Data Section

A. Ventura and F. Cannata
ENEA and INFN, Bologna, Italy

RC 12421: **Nuclear level densities at high excitation energies**

RECURSIVE METHOD

F.C. Williams Jr., *Nucl. Phys.* **A133**, 33 (1969)

INPUT: Single-particle level scheme

A mathematically exact recursive method is used for the solution of the problem within Fermi gas model. No residual interaction is considered. The TotSTADE code for recursive state density (SD) calculations was tested and released: "Nuclear state density calculations: An exact recursive approach", *Comp. Phys. Comm.* ***150*** *(2003) 43-52*

Proton system Z=40, Zr-82

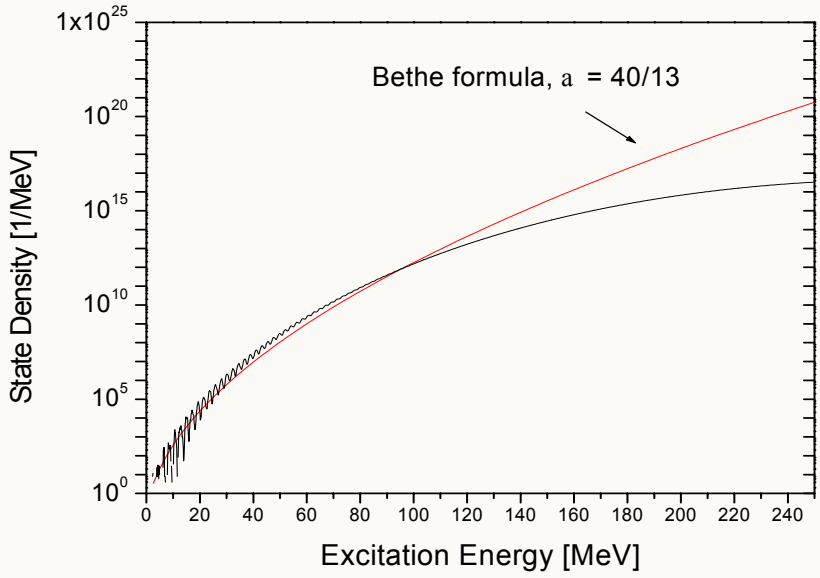

Zr-82, Total SD

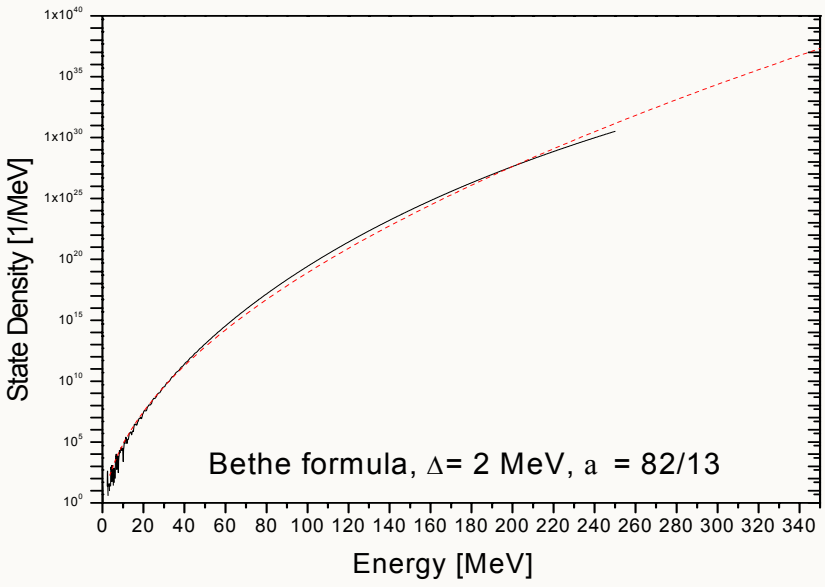

HIGH ENERGY SD

The recursive method was used to study high energy behavior of the intrinsic state density for near to magic zirconium and rutenium nuclei up to 250 MeV. It was shown that Bethe formula fails to describe the SD corresponding to neutron and proton systems above 140 MeV. However Bethe formula describes much better than expected the total state density behavior up to 250 MeV

Sensitivity to SPL

The sensitivity of the obtained nuclear level density to the number of single-particle levels included in the calculation was analyzed. It was found that bound neutron single particle levels ($E<0$) and quasi-bound proton single particle levels (below Coulomb barrier) are enough to be used as input single particle states for microscopic state density calculations up to 250 MeV

MONTE CARLO METHOD

Based on the Metropolis algorithm† as proposed by Cerf ‡ in order to avoid an exhaustive counting of the combinations

† N. Metropolis *et al*, *J.Chem.Phys.***21**(1953) 1087

‡ N. Cerf, *Phys.Rev.***C49**(1994) 852

Normalization by recursive state density calculation.

Allow to consider pairing interaction.

TOTAL LD CALCULATION

$$\omega(E,M,\pi) = \sum_{\pi_i\pi_c=\pi}\int_0^{\infty} dE_i \sum_{M_i+M_c=M} \omega_i(E_i,M_i,\pi_i) \times\omega_c(E-E_i,M_c,\pi_c),$$

$$\omega_{coll.}(E,\pi) = \sum_{J=0}^{J_{max}(\pi)} (2J+1)\sum_c \delta(E-E_c(J,\pi))$$

$$\omega_{coll.}(E,M,\pi) = \omega_{coll.}(E,\pi)\, f_{coll.}(M,\pi),$$

$$\rho(E,J,\pi) = \omega(E,M=J,\pi) - \omega(E,M=J+1,\pi)$$

Sm isotopes LD

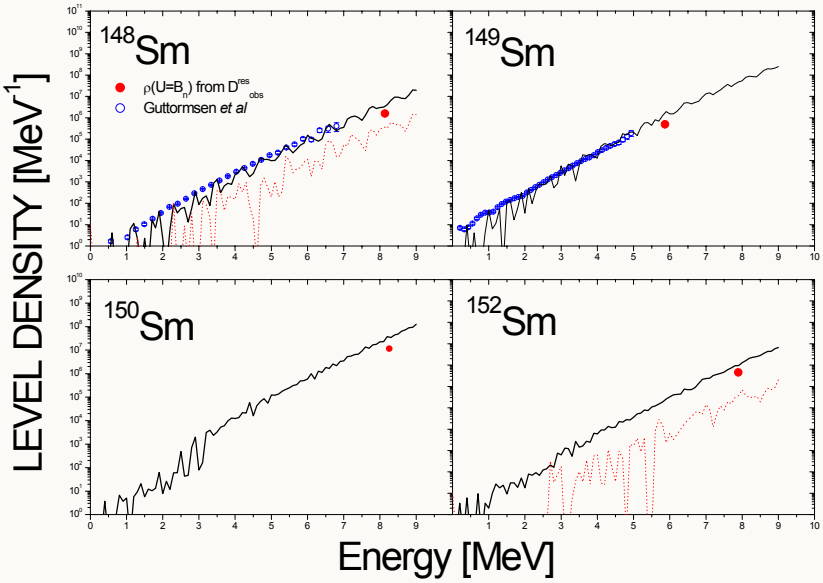

Summary for Sm isotopes

- A new code was developed and tested for intrinsic level density calculations by Monte Carlo sampling of excited configurations.

- A methodology for estimation of the collective enhancement of the LD at B_n for Sm isotopes is proposed based on IBM description of the low lying levels.

- Total level density for samarium isotopes 148,149,150 and 152 was calculated by convolution of the collective and intrinsic state densities. A good agreement of the available experimental data below 10 MeV was achieved.

Appendix 3.6

BNL- NNDC contribution to RIPL-3

M. Herman, P. Oblozinsky and S. Mughabghab

BNL-NNDC contribution to RIPL-3

M.Herman, P. Oblozinsky, S. Mughabghab

Brookhaven National Laboratory

e-mail: mwherman@bnl.gov

BNL-NNDC proposed work plan

- Large scale calculations with EMPIRE-II in order to identify weak points of RIPL-2
- Evaluation of neutron resonance spacings for all isotopes with adequate experimental data (new BNL-325 by S. Mughabghab)
- Determination of parameters for EMPIRE-specific level densities using new resonance spacings (**including uncertainties** for a-parameter)

Proposed work plan (cont.)

- Systematics of parameters for EMPIRE-specific level densities
- Stand-alone version of the EMPIRE-specific level densities routine (RIPL-3/ModLib)
- Implementation of the new gamma-ray strength functions in hot nuclei (RIPL-3) in the EMPIRE code
- Large scale calculations with EMPIRE-II in order to validate RIPL-3 data

Relation to RIPL-3 goals

- EMPIRE-specific level densities account for:
  - non-adiabatic collective enhancements due to nuclear vibration and rotation => extension of l.d. to higher energies
  - rotation induced deformation through spin-dependent moments of inertia => extension of l.d. to higher spins (HI reactions)
- gamma-ray strength functions in hot nuclei => extension to higher energies

EMPIRE-specific level densities

- Features:
  - Collective enhancements due to nuclear vibration and rotation.
  - Super-fluid model below critical excitation energy (GSF)
  - Fermi gas model above critical excitation energy (FG)
  - Rotation induced deformation (spin dependent) => moments of inertia

EMPIRE-specific lev. dens. (FG)

- Prolate nuclei

$$\rho(E,J,\pi) = \frac{1}{16\sqrt{6\pi}}\left(\frac{\hbar^2}{\Im_{\parallel}}\right)^{\frac{1}{2}} a^{1/4} \sum_{K=-J}^{J}\left(U-\frac{\hbar^2K^2}{2\Im_{eff}}\right)^{-\frac{5}{4}} \exp\left\{2\left[a\left(U-\frac{\hbar^2K^2}{2\Im_{eff}}\right)\right]^{\frac{1}{2}}\right\}.$$

EMPIRE-specific lev. dens. (FG)

- Oblate nuclei

$$\rho(E,J,\pi) = \frac{1}{16\sqrt{6\pi}}\left(\frac{\hbar^2}{\Im_{\parallel}}\right)^{\frac{1}{2}} a^{1/4} \sum_{K=-J}^{J}\left(U-\frac{\hbar^2\left[J\left(J+1\right)-K^2\right]}{2|\Im_{eff}|}\right)^{-\frac{5}{4}} \exp\left\{2\left[a\left(U-\frac{\hbar^2\left[J\left(J+1\right)-K^2\right]}{2|\Im_{eff}|}\right)\right]^{\frac{1}{2}}\right\}.$$

EMPIRE-specific lev. dens.(FG)

K - spin projection,
$\Im_{eff}$ - effective moment of inertia
defined in terms of perpendicular $\Im_{\parallel}$and parallel $\Im_{\perp}$moments

$$\frac{1}{\Im_{eff}} = \frac{1}{\Im_{\parallel}} - \frac{1}{\Im_{\perp}}.$$

EMPIRE-specific lev. dens. (FG)

- Rotational enhancement automatically taken into account.
- Vibrational enhancement

$$K_{vib} = exp\left\{1.7\left(\frac{3m_0A}{4\pi h^2 S_{drop}}\right)^{2/3} T^{4/3}\right\}$$

with $S_{drop} = 17/4\pi r_{2_0}$ and $r_0 = 1.26$.

- Rotational and vibrational enhancements are damped with increasing energy

Super-fluid (GSF) lev. dens.

- Used below critical energy
- pairing gap $\Delta = 12/\sqrt{A}$
- critical temperature T_{crt} is $T_{crt} = 0.567\Delta$

Super-fluid (BCS) lev. dens.

- The critical value of the level density parameter a is determined by the iteration procedure

$$a_{crt}^{(0)} = \widetilde{a}\,(1 + \gamma\delta_W)$$

$$U^{(n)} = a_{crt}^{(n)} T_{crt}^2$$

$$a_{crt}^{(n+1)} = \widetilde{a}\left[1 + \frac{\delta_W}{U^{(n)}}\left(1 - \exp\left(-\gamma U^{(n)}\right)\right)\right]$$

$\widetilde{a}$ is the asymptotic value of a

Super-fluid (GSF) lev. dens.

Critical values of relevant quantities

$$E_{cond} = 1.5 a_{crt}\Delta^2/\pi^2$$

$$U_{crt} = a_{crt}T_{crt}^2 + E_{cond}$$

$$Det_{crt} = \left(\frac{12}{\sqrt{\pi}}\right)^2 a_{crt}^3 T_{crt}^5$$

$$S_{crt} = 2a_{crt}T_{crt}$$

Super-fluid (GSF) lev. dens.

At excitation energies below U_{crt} we define the parameter $\varphi = \sqrt{1 - U/U_{crt}}$, which allows to express all thermodynamical quantities in terms of their critical values

$$T = 2T_{crt}\varphi \ln^{-1}\left(\frac{\varphi+1}{1-\varphi}\right)$$

$$S = S_{crt}T_{crt}(1-\varphi^2)/T$$

$$Det = Det_{crt}(1-\varphi^2)(1+\varphi^2)^2$$

Super-fluid (GSF) lev. dens.

The parallel and orthogonal moments of inertia below the critical temperature T_{crt} are

$$\Im_{\parallel}^{BCS} = \Im_{\parallel}T_{crt}(1-\varphi^2)/T$$

and

$$\Im_{\perp}^{BCS} = \frac{1}{3}\Im_{\perp} + \frac{2}{3}\Im_{\perp}T_{crt}(1-\varphi^2)/T$$

Super-fluid (GSF) lev. dens.

Using these results squares of the effective spin cut-off parameters are

$$\sigma^2_{eff} = \Im^{BCS}_{\parallel} T \qquad for\ \alpha_2 < 0.005\,,$$
$$\sigma^2_{eff} = \left(\Im^{BCS}_{\parallel}\right)^{1/3} \left(\Im^{BCS}_{\perp}\right)^{2/3} T \qquad for\ \alpha_2 > 0.005\,,$$

with α_2 ground state deformation.

Super-fluid (GSF) lev. dens.

$$\rho_{BCS}(U,J) = \frac{2J+1}{2\sqrt{2\pi}\sigma^3_{eff}\sqrt{Det}} \exp\left(\frac{S - J(J+1)}{2\sigma^2_{eff}}\right)$$

Correcting for rotational and vibrational effects in the non-adiabatic mode (i.e., including their damping with increasing temperature)

$$\rho(U,J) = \rho_{BCS}(U,J) Q^{BCS}_{rot} K_{rot} Q_{vib} K_{vib}\,.$$

Super-fluid (GSF) lev. dens.

The rotational enhancement is

$$K_{rot} = \Im_{\perp} T$$

and is damped with

$$Q_{rot}^{BCS} = 1 - Q_{rot}\left(1 - \frac{1}{\Im_{\perp} T}\right),$$

EMPIRE-specific a-param.

(i) EMPIRE-specific:

- a energy dependent following Ignatyuk et al.

$$a(U) = \tilde{a}[1 + f(U)\frac{\delta_W}{U}]$$

with

$$f(U) = 1 - exp(-\gamma U)$$

δ_W being the shell correction

EMPIRE-specific a-param.

and $\widetilde{a}$ the asymptotic value of the a-parameter

$$\widetilde{a} = \eta A + \zeta A^{2/3} F_{surf}(R_{max}/R_{min})$$

includes deformation dependent term F_{surf}

EMPIRE-specific systematics

- experimental values extracted from fitting D_{obs}
  - Nix-Moeller shell-corrections:

$Z < 85$		$Z \geq 85$	
$\eta =$	0.094431	$\eta =$	0.117113
$\xi =$	-0.08014	$\xi =$	-0.09939
$\gamma =$	0.075594	$\gamma =$	0.094447

EMPIRE-specific systematics

- Myers-Swiatecki shell-corrections:

$Z < 85$		$Z \geq 85$	
$\eta =$	0.052268	$\eta =$	0.067645
$\xi =$	0.13395	$\xi =$	0.173358
$\gamma =$	0.093955	$\gamma =$	0.121465

Appendix 3.7

LANL contributions to the RIPL-3 project

P. Talou

LANL Contributions to the RIPL-3 Project

P. Talou, T-16, Nuclear Physics Group
Los Alamos National Laboratory

- Model input parameters for high-energy evaluations
- Work on Pu-239 and suite of Uranium isotopes
- Evaluation of n+Am-242m,g for AFCI
- Prompt fission neutron spectrum calculations using CEM2k intranuclear cascade code
- FIGARO experimental data on (n,n'g) outgoing neutron spectra [Haight, Rochman, LANSCE]
- Covariance data from nuclear model calculations
- Link with the ModLib effort

Model input parameters for high-energy evaluations

Suite of Uranium isotopes (232,233,234,235,238), Pu-239, Am-242m & experience from the development of the LA150 library.

- Optical model parameters used in the coupled-channels calculations up to 200 MeV.
- Discrete levels and rotational-vibrational coupling schemes
- Level density parameters for various nuclei away from the beta-valley of stability.
- Fission channel: Bjornholm-Lynn double-humped fission barrier, uncoupled oscillators. Fission barrier parameters, discrete fission transition states, symmetry breaking enhancement factors.
- charged-particle emission

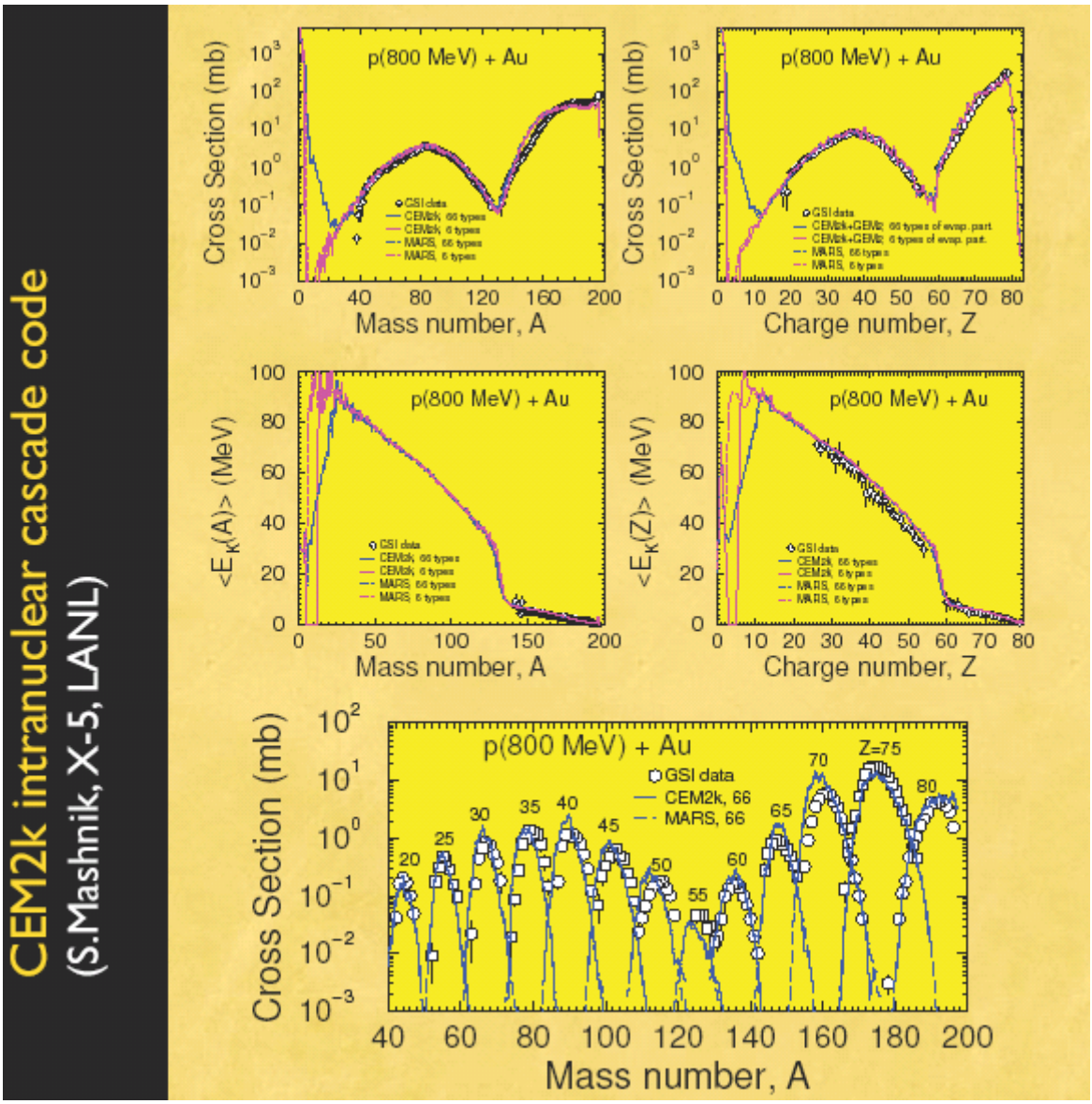
CEM2k intranuclear cascade code
(S.Mashnik, X-5, LANL)
p(800 MeV) + Au
Cross Section (mb)
Mass number, A
Charge number, Z
<E_K(A)> (MeV)
<E_K(Z)> (MeV)
GSI data
CEM2k, 66
MARS, 66
Z=75
20
25
30
35
40
45
50
55
60
65
70
80

Calculation of the prompt neutron fission spectrum from 20 to 150 MeV.

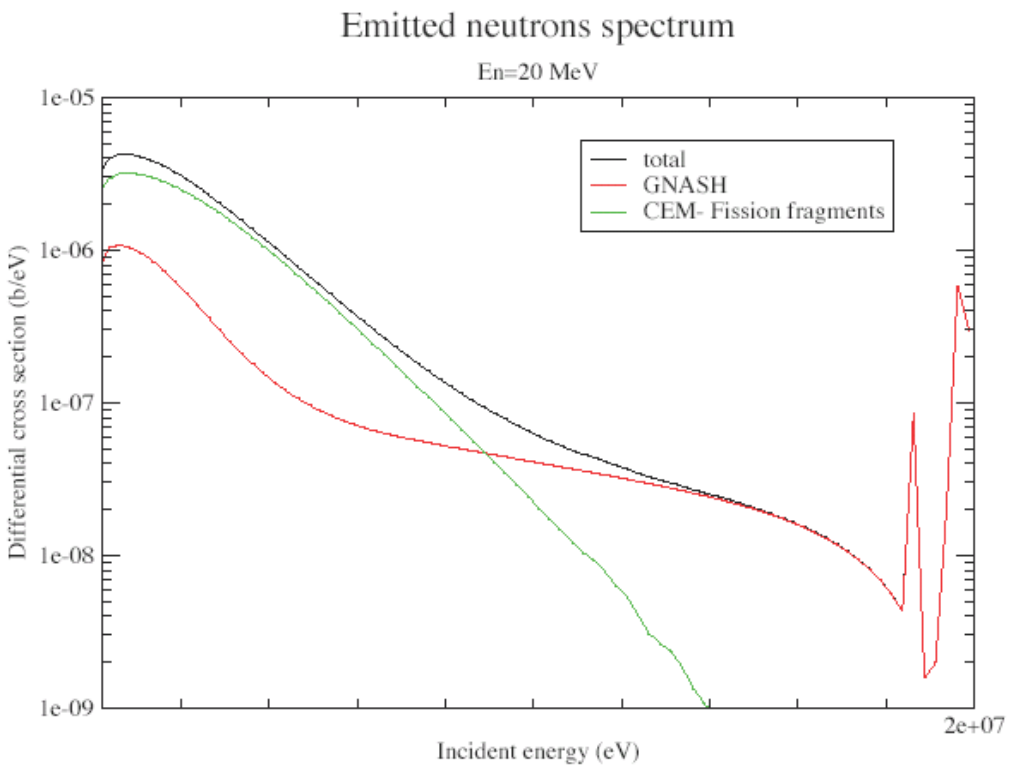

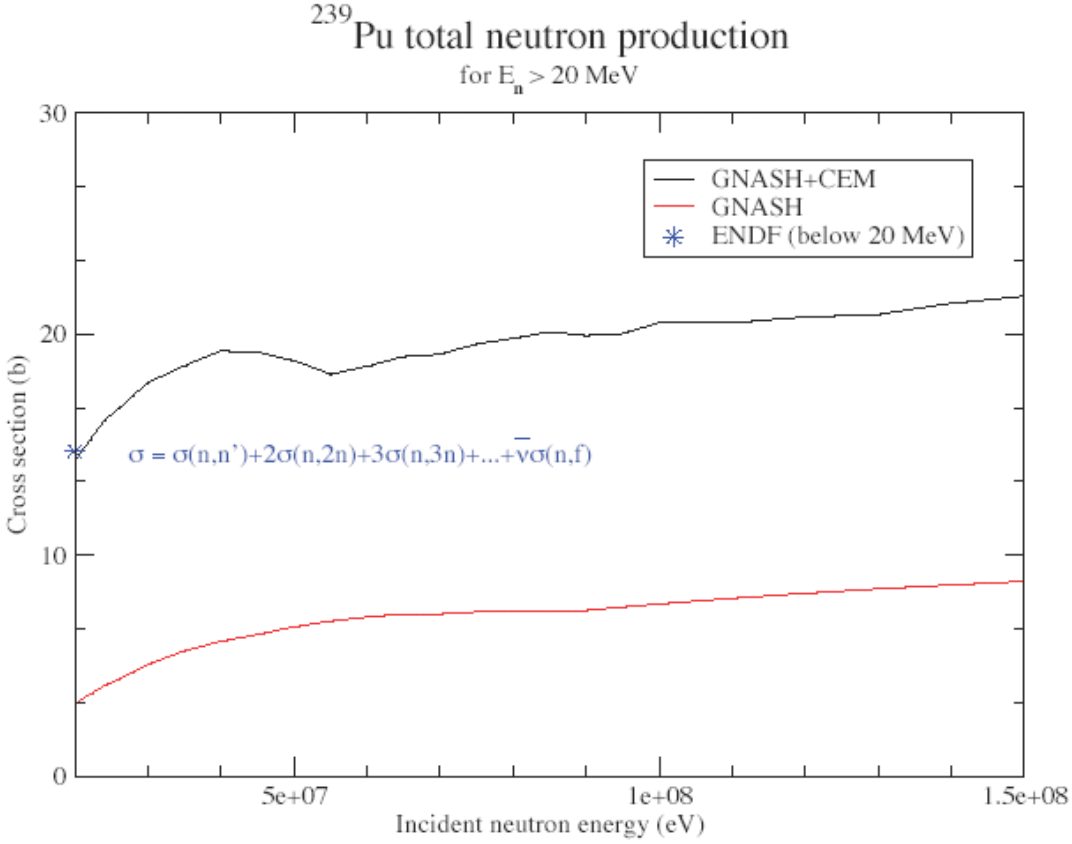

Work on Americium isotopes for the Advanced Fuel Cycle Initiative

Example: $n+^{242m}Am$

In collaboration with A.Koning (EuroTrans-AFCI Agreement)

Metastable state: 5-; 48.6 keV; 141 years
Ground-state: 1-; 16.02 hours

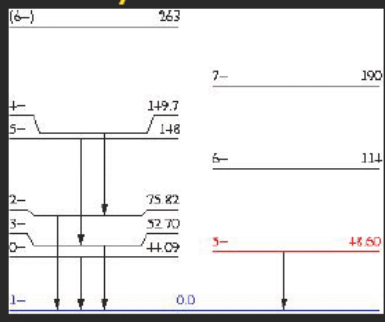

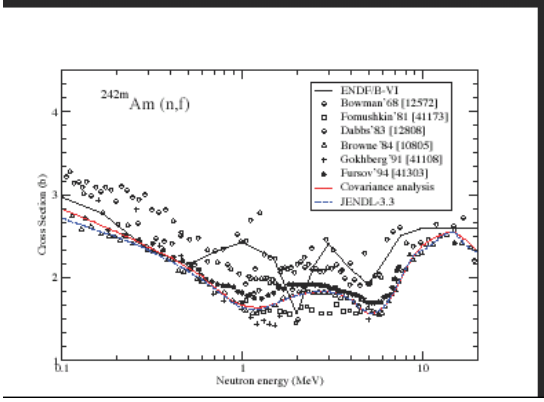

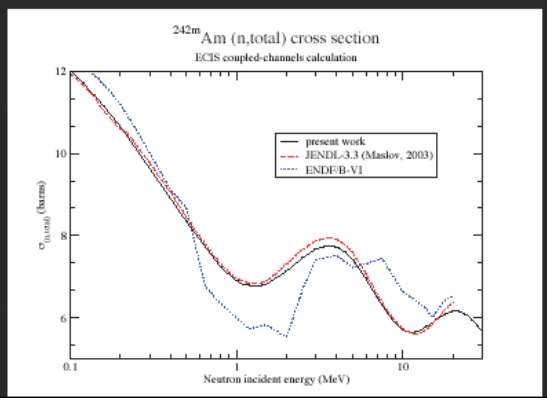

FIGARO measures neutron emission spectra in neutron-induced reactions by double time of flight

- FIGARO – Fast-neutron-Induced Gamma-ray Observer
- Incident neutron energy determined by time of flight from source
- Outgoing neutron energy determined by time of flight from sample – triggered by gamma ray

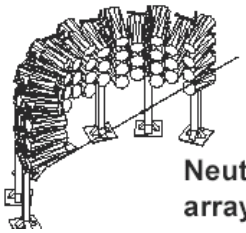

Neutron detector array

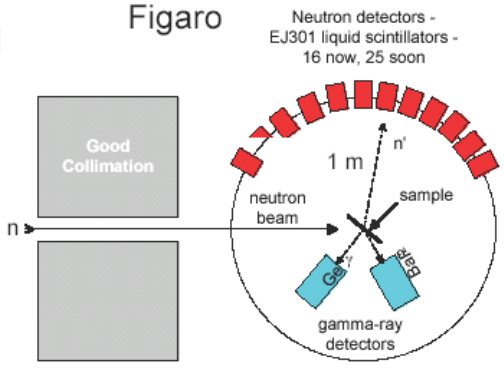

22 m flight path at WNR/LANSCE

^{nat}Ni(n,n'γ): EMPIRE, with modified level density parameters, reproduces the data quite well.

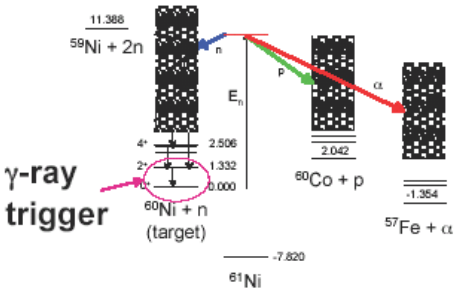

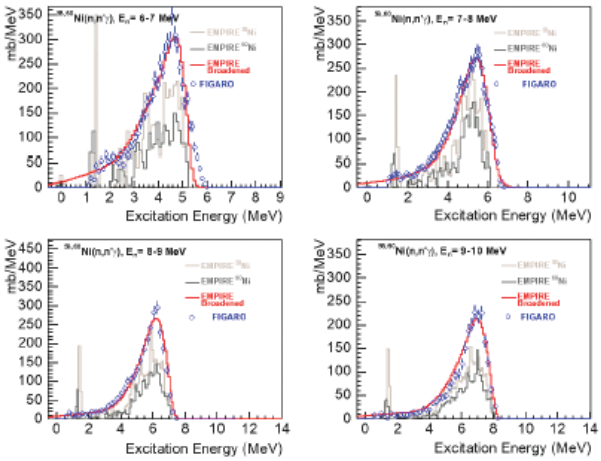

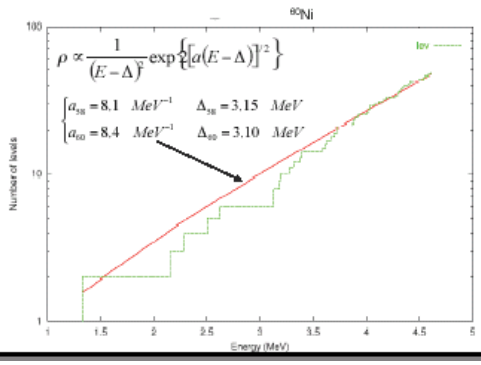

Neutron emission spectra triggered by 2+ -> g.s. γ-ray transitions in ^{58}Ni and ^{60}Ni

Goals of FIGARO research include data for evaluations and basic science of nuclear reactions

- Neutron- emission spectra from (n,n') and other reactions for evaluations
- Triggering on different gamma rays restricts range of angular momentum range of states in continuum -> handle on angular momentum dependence of level densities

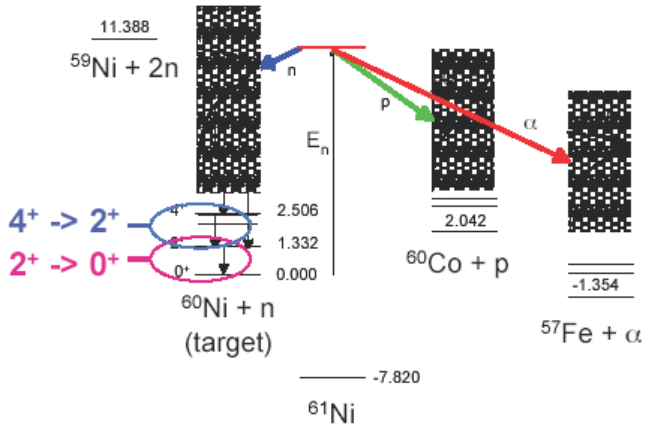

Covariance Data from Nuclear Models

"Covariance Matrix Calculated from Nuclear Models"
T.Kawano, K.Kamitsubo, T.Iwamoto and Y.Kanda
Proc. of the Specialists' Meeting on Covariance Data, July 15-16, 1993, Tokai, Japan

$$\begin{aligned}\mathbf{x_1} &= \mathbf{x_0} + \mathbf{P}\mathbf{C}^t\mathbf{V}^{-1}\left(\mathbf{y} - \mathbf{f}(\mathbf{x_0})\right) \\ &= \mathbf{x_0} + \mathbf{X}\mathbf{C}^t\left(\mathbf{C}\mathbf{X}\mathbf{C}^t + \mathbf{V}\right)^{-1}\left(\mathbf{y} - \mathbf{f}(\mathbf{x_0})\right) \\ \mathbf{P} &= \left(\mathbf{X}^{-1} + \mathbf{C}^t\mathbf{V}^{-1}\mathbf{C}\right)^{-1} \\ &= \mathbf{X} - \mathbf{X}\mathbf{C}^t\left(\mathbf{C}\mathbf{X}\mathbf{C}^t + \mathbf{V}\right)^{-1}\mathbf{C}\mathbf{X}\end{aligned}$$

$\mathbf{x} = (x_1, x_2, \ldots, x_m)^t$ is a model parameter vector
$\mathbf{y} = (y_1, y_2, \ldots, y_n)^t$ is an experimental data vector
$\mathbf{X} = \left\langle (\mathbf{x} - \mathbf{x_0}), (\mathbf{x} - \mathbf{x_0})^t \right\rangle$ is the *prior* covariance matrix for the model parameters (an m-dimensional normal distribution with <X>=x_0, where x_0 is a prior parameter vector)

($\mathbf{x}_1$,**P**) *posterior* parameter vector and its covariance matrix

***C** is a **sensitivity matrix** which is obtained by numerical derivatives of the model calculations around the parameters.*

Covariance matrix of evaluated nuclear data: $\mathbf{M} = \mathbf{C}\mathbf{P}\mathbf{C}^t$

ModLib: International Collaboration on Nuclear Reaction Codes

Development of a library of Fortran95 modules that can be used in existing (and future) nuclear reaction codes such as Empire, Talys, Mcgnash.

Many advantages.

Release of the first version of the library by the end of 2004: about 6-7 modules to be included + ENDF checking modules from C.Dunford.

Obvious relation with RIPL databases development.

→ Interfaces and retrieval tools.

Nuclear Data Section
International Atomic Energy Agency
P.O. Box 100
A-1400 Vienna
Austria

e-mail: services@iaeand.iaea.org
fax: (43-1) 26007
telephone: (43-1) 2600-21710

Online: TELNET or FTP: iaeand.iaea.org
username: IAEANDS for interactive Nuclear Data Information System
usernames: ANONYMOUS for FTP file transfer;
FENDL2 for FTP file transfer of FENDL-2.0;
RIPL for FTP file transfer of RIPL.
NDSONL for FTP access to files sent to NDIS “open” area.
Web: http://www-nds.iaea.org